Cerebral Cortex, 2020;00: 1–18

doi: 10.1093/cercor/bhaa356
Original Article

ORIGINAL ARTICLE

Abnormalities of Cortical Sources of Resting State Alpha Electroencephalographic Rhythms are Related to Education Attainment in Cognitively Unimpaired Seniors and Patients with Alzheimer's Disease and Amnesic Mild Cognitive Impairment

Claudio Babiloni[1,2], Raffaele Ferri[3], Giuseppe Noce[4], Roberta Lizio[4], Susanna Lopez[5], Ivan Lorenzo[3], Andrea Panzavolta[1], Andrea Soricelli[4,6], Flavio Nobili[7,8], Dario Arnaldi[7,8], Francesco Famà[8], Francesco Orzi[9], Carla Buttinelli[9], Franco Giubilei[9], Virginia Cipollini[9], Moira Marizzoni[10], Bahar Güntekin[11,12], Tuba Aktürk[12], Lutfu Hanoğlu[13], Görsev Yener[14,15], Yağmur Özbek[15], Fabrizio Stocchi[16], Laura Vacca[16], Giovanni B. Frisoni[10,17] and Claudio Del Percio[1]

[1]Department of Physiology and Pharmacology "Vittorio Erspamer", Sapienza University of Rome, Rome, Italy, [2]San Raffaele of Cassino, Cassino, Italy, [3]Oasi Research Institute—IRCCS, Troina, Italy, [4]IRCCS SDN, Napoli, Italy, [5]Nephrology, Dialysis and Transplantation Unit, Department of Emergency and Organ Transplantation, Aldo Moro University of Bari, Bari, Italy, [6]Department of Motor Sciences and Healthiness, University of Naples Parthenope, Naples, Italy, [7]Clinica Neurologica, IRCCS Ospedale Policlinico San Martino, Genova, Italy, [8]Dipartimento di Neuroscienze, Oftalmologia, Genetica, Riabilitazione e Scienze Materno-infantili (DiNOGMI), Università di Genova, Italy, [9]Department of Neuroscience, Mental Health and Sensory Organs, Sapienza University of Rome, Rome, Italy, [10]Laboratory of Alzheimer's Neuroimaging and Epidemiology, IRCCS Istituto Centro San Giovanni di Dio Fatebenefratelli, Brescia, Italy, [11]Department of Biophysics, School of Medicine, Istanbul Medipol University, Istanbul, Turkey, [12]REMER, Clinical Electrophysiology, Neuroimaging and Neuromodulation Lab., Istanbul Medipol University, Istanbul, Turkey, [13]Department of Neurology, School of Medicine, Istanbul Medipol University, Istanbul, Turkey, [14]Izmir Biomedicine and Genome Center, Dokuz Eylul University Health Campus, Izmir, Turkey, [15]Department of Neurosciences, Institute of Health Sciences, Dokuz Eylul University, Izmir, Turkey, [16]Institute for Research and Medical Care, IRCCS San Raffaele Pisana, Rome, Italy and [17]Memory Clinic and LANVIE—Laboratory of Neuroimaging of Aging, University Hospitals and University of Geneva, Geneva, Switzerland

Address correspondence to Prof. Claudio Babiloni, Ph.D. Department of Physiology and Pharmacology "V. Erspamer", Sapienza University of Rome, P. le A. Moro 5, 00185 Rome, Italy. Email: claudio.babiloni@uniroma1.it.

Abstract

In normal old (Nold) and Alzheimer's disease (AD) persons, a high cognitive reserve (CR) makes them more resistant and resilient to brain neuropathology and neurodegeneration. Here, we tested whether these effects may affect neurophysiological oscillatory mechanisms generating dominant resting state electroencephalographic (rsEEG) alpha rhythms in Nold and patients with mild cognitive impairment (MCI) due to AD (ADMCI). Data in 60 Nold and 70 ADMCI participants, stratified in higher (Edu+) and lower (Edu–) educational attainment subgroups, were available in an Italian–Turkish archive. The subgroups were matched for age, gender, and education. RsEEG cortical sources were estimated by eLORETA freeware. As compared to the Nold-Edu– subgroup, the Nold-Edu+ subgroup showed greater alpha source activations topographically widespread. On the contrary, in relation to the ADMCI-Edu– subgroup, the ADMCI-Edu+ subgroup displayed lower alpha source activations topographically widespread. Furthermore, the 2 ADMCI subgroups had matched cerebrospinal AD diagnostic biomarkers, brain gray–white matter measures, and neuropsychological scores. The current findings suggest that a high CR may be related to changes in rsEEG alpha rhythms in Nold and ADMCI persons. These changes may underlie *neuroprotective* effects in Nold seniors and subtend functional *compensatory* mechanisms unrelated to brain structure alterations in ADMCI patients.

Key words: aging, education attainment, exact low-resolution brain electromagnetic source tomography (eLORETA), mild cognitive impairment due to Alzheimer's disease (ADMCI), resting state electroencephalographic (rsEEG) rhythms

Introduction

Cognitive reserve (CR) is a concept used to explain individual differences in the way cerebral networks underlying cognitive functions (i.e., attention, memory, etc.) are resistant and resilient over time to neuropathological processes including those associated with Alzheimer's disease with dementia (ADD) (Stern et al. 2018). CR may be fruitfully indexed by measures of premorbid intelligence, vocabulary skills, education attainment, job demands in the life span, and socio-affective activities (Arenaza-Urquijo et al. 2015; Stern et al. 2018).

Nonlinear relationships between neuropathological progression and clinical symptoms in ADD patients with high CR subtend at least 2 underlying cerebral mechanisms. The so-called "neuroprotective mechanism" was supposed to postpone the onset of clinical manifestations in ADD patients with high CR (Valenzuela and Sachdev 2006; Garibotto et al. 2008; Reed et al. 2010; Buchman and Bennett 2012; Stern 2012; Zahodne et al. 2013, 2015; Bennett et al. 2014; Morbelli and Nobili 2014; Arenaza-Urquijo and Vemuri 2018; Stern et al. 2018; Hampel et al. 2019), while the "compensatory mechanism" may reduce the expected impact of the AD neuropathology on the clinical status in ADD patients with high CR (Stern et al. 2018). Such a compensatory mechanism may ensure similar cognitive performances in ADD patients with high and low CR although those with high CR typically show: (1) more reduced cerebral blood flow (Stern et al. 1995), (2) higher brain atrophy and microstructural changes measured by magnetic resonance imaging (MRI; Querbes et al. 2009; Sole-Padulles et al. 2009; Teipel et al. 2009; Liu et al. 2012; van Loenhoud et al. 2017), (3) lower brain metabolism in AD vulnerable regions measured by [18F]fluoro-deoxy-glucose-positron emission tomography (FDG-PET; Pietrini et al. 1999; Perneczky et al. 2006; Garibotto et al. 2008; Morbelli et al. 2013; Morbelli and Nobili 2014), and (4) higher cerebral levels of amyloid and tau measured by PET imaging (Roe et al. 2007; Rentz et al. 2017).

The same compensatory mechanisms of the CR are supposed to operate in prodromal ADMCI. As compared to ADMCI patients with low CR, those with high CR showed similar cognitive deficits despite greater FDG-PET hypometabolism in the precuneus (Garibotto et al. 2008; Franzmeier, Göttler, et al. 2017a; Franzmeier, Duering, et al. 2017b) and temporo-parietal associative cortical areas (Garibotto et al. 2008). These CR effects were stronger in ADMCI patients who converted to ADD than the stable ones (Morbelli et al. 2013).

Among several parallel neurobiological mechanisms (Stern et al. 2018), CR may exert its influence on brain functions by changes in rsEEG rhythms. Previous rsEEG studies in young subjects and normal old (Nold) seniors reported that a high CR (education attainment and verbal intelligent quotient) was associated with an enhanced functional coupling of alpha rhythms (8–12 Hz) topographically widespread (Fleck et al. 2017, 2019). In another rsEEG study carried out in seniors with subjective memory complaints (SMC), we showed that in the participants with negative amyloid-β amyPET scans, the high CR was related to more ample alpha rhythms in posterior areas, possibly reflecting a neuroprotective mechanism (Babiloni, Lopez, et al. 2020a). On the contrary, in the amyPET positive SMC participants, the high CR was related to less ample posterior alpha rhythms, possibly reflecting a compensatory mechanism preserving the cognitive status despite the alpha abnormalities (Babiloni, Lopez, et al. 2020a).

Noteworthy, posterior rsEEG alpha rhythms are affected by the AD even at prodromal stages and may be related to the integrity of ascending cholinergic neuromodulation systems (Wan et al. 2019). Previous rsEEG studies showed that ADMCI patients were characterized by lower alpha source activations and higher delta (<4 Hz) and theta (4–8 Hz) source activations in association with abnormalities in brain structure and alterations in functional connectivity within cortical default mode network (Babiloni, Binetti et al. 2006; Babiloni et al. 2013, 2015, 2018a, 2018b; Galluzzi et al. 2016; Jovicich et al. 2019; Marizzoni et al. 2019). These abnormalities in alpha source activations also exhibited peculiar features when compared to those observed in patients with Parkinson's and Lewy Body diseases presenting cognitive deficits from MCI to dementia (Babiloni, Del Percio, Lizio, Noce, Lopez, et al. 2017a; Babiloni, Del Percio, Lizio, Noce, Cordone, et al. 2017b; Babiloni et al. 2018a, 2018b).

Summarizing, our previous studies reported that a high CR (proxy: education attainment) was associated with dominant rsEEG alpha rhythms having (1) greater magnitude in the SMC

Table 1 Mean values (±standard error of the mean, SE) of the demographic and clinical data as well as the results of their statistical comparisons ($P < 0.05$) in the groups of normal old (Nold) seniors ($N = 60$) and patients with ADMCI ($N = 70$)

Demographic and clinical data in Nold and ADMCI			
	Nold	ADMCI	Statistical analysis
N	60	70	
Age	69.0 ± 0.9 SE	69.5 ± 0.8 SE	*T*-test: 0.6
Gender (M/F)	23/37	27/43	Fisher test: 1.0
Education	9.8 ± 0.6 SE	10.8 ± 0.5 SE	*T*-test: 0.2
MMSE	28.4 ± 0.1 SE	25.3 ± 0.3 SE	Mann–Whitney *U* test: $P < 0.00001$

Note: MMSE, Minimental State Evaluation; M/F, males/females.

individuals unaffected by AD and (2) lower magnitude in the SMC individuals with preclinical Alzheimer's neuropathology (Babiloni, Lopez, et al. 2020a). Furthermore, rsEEG alpha source activations were lower in ADMCI patients as compared to several control groups (Galluzzi et al. 2016; Babiloni, Del Percio, Lizio, Noce, Lopez, et al. 2017a; Babiloni, Del Percio, Lizio, Noce, Cordone, et al. 2017b; Babiloni et al. 2018a, 2018b; Jovicich et al. 2019). Keeping in mind those previous data, here we hypothesize that as compared to the low CR, the high CR may be associated with (1) greater rsEEG alpha source activations in Nold (no SMC) individuals as a potential neuroprotective mechanism and (2) reduced rsEEG alpha source activations in ADMCI patients subtending a compensatory mechanism mitigating the effects of that reduction on their clinical status.

Materials and Methods

Participants

To test the study hypotheses, we used the data of a national archive, formed by clinical, neuropsychological, anthropometric, genetic, cerebrospinal fluid (CSF), MRI, and rsEEG data in 60 Nold and 70 ADMCI subjects. These subjects were recruited by the following Italian and Turkish clinical units: the Sapienza University of Rome (Italy), Institute for Research and Evidence-based Care (IRCCS) "Fatebenefratelli" of Brescia (Italy), IRCCS SDN of Naples (Italy), IRCCS Oasi Maria SS of Troina (Italy), IRCCS Ospedale Policlinico San Martino and DINOGMI (University of Genova, Italy), Hospital San Raffaele of Cassino (Italy), IRCCS San Raffaele Pisana of Rome (Italy), and Medipol University of Istanbul (Turkey).

The 2 groups (i.e., Nold and ADMCI) were carefully matched for age, gender, and education (i.e., the mean values of age, gender, and education were not different between these groups). Table 1 summarizes the most relevant demographic (i.e., age, gender, and educational attainment) and clinical (i.e., minimental state evaluation, MMSE, score) features of the Nold and ADMCI groups. Furthermore, Table 1 reports the results of the presence or absence of statistically significant differences ($P < 0.05$) between the 2 groups for age (*T*-test), gender (Fisher test), educational attainment (*T*-test), and MMSE score (Mann–Whitney *U* test). As expected, a statistically significant difference was found for the MMSE score ($P < 0.00001$), showing a higher score in the Nold than the ADMCI group. On the contrary, no statistically significant differences were found for the age, gender, and education attainment between the groups ($P > 0.05$).

Local institutional Ethics Committee approved the present observational study. All experiments were performed with the informed and overt consent of each participant or caregiver, in line with the Code of Ethics of the World Medical Association (Declaration of Helsinki) and the standards established by the local Institutional Review Board.

To test the effect of educational attainment on the rsEEG source activations, the enrolled Nold seniors and ADMCI patients were stratified in 2 subgroups, respectively, based on the low (years of education ≤ 8; Nold-Edu–, $N = 30$; ADMCI-Edu–, $N = 35$) and high (years of education >8; Nold-Edu+, $N = 30$; ADMCI-Edu+, $N = 35$) educational level. Table 2 summarizes the most relevant demographic (i.e., age, gender, and education attainment) and clinical (i.e., MMSE score) features of the Nold-Edu–, Nold-Edu+, ADMCI-Edu–, and ADMCI-Edu+ subgroups. Furthermore, Table 2 reports the results of the presence or absence of statistically significant differences ($P < 0.05$) between the Edu– and Edu+ subgroups for both Nold and ADMCI groups (i.e., Nold-Edu– vs. Nold-Edu+, ADMCI-Edu– vs. ADMCI-Edu+) for the age (*T*-test), gender (Fisher test), education attainment (*T*-test), and MMSE score (Mann–Whitney *U* test). As expected, and based on the stratification criterion, a statistically significant difference in education was found between the Edu– and Edu+ subgroups for both Nold and ADD groups considered separately ($P < 0.000001$). On the contrary, no statistically significant differences were found for the age, gender, and MMSE score between the Edu– and Edu+ subgroups for both Nold and ADD groups, considered separately ($P > 0.05$).

Diagnostic Criteria

The status of the ADMCI was based on the "positivity" to one or more of the following biomarkers: Aβ1–42/phospho-tau ratio in the CSF, FDG-PET, and structural MRI of the hippocampus, parietal, temporal, and posterior cingulate regions (Albert et al. 2011). The "positivity" was judged by the physicians in charge of releasing the clinical diagnosis to the patients, according to the local diagnostic routine of the participating clinical Units.

The clinical inclusion criteria of the ADMCI patients were as follows: (1) age of 55–90 years; (2) reported memory complaints by the patient and/or a relative; (3) MMSE score of 24 or higher; (4) Clinical Dementia Rating (CDR) score of 0.5 (Morris 1993); (5) logical memory test (Wechsler 1987) score of 1.5 standard deviations (SD) below the mean adjusted for age; the cognitive deficits did not significantly interfere with the functional independence in the activities of the daily living; (6) Geriatric Depression Scale (15-item GDS; Brown and Schinka 2005) score of 5 or lower; (7) modified Hachinski ischemia (Rosen et al. 1980) score of 4 or lower and education of 5 years or higher; and (8) single or multidomain MCI status.

The clinical exclusion criteria of the ADMCI patients were as follows: (1) other significant systemic, psychiatric, neurological

Table 2 Mean values (±SE) of the demographic and clinical data as well as the results of their statistical comparisons ($P < 0.05$) in the groups of Nold seniors and ADMCI patients stratified according to the low (years of education ≤ 8; Nold-Edu+, $N = 30$; ADMCI-Edu+, $N = 35$) or high (years of education > 8; Nold-Edu+, $N = 30$; ADMCI-Edu+, $N = 35$) educational attainment

Demographic and clinical data in Nold-Edu–, Nold-Edu+, ADMCI-Edu–, and ADMCI-Edu+					
	Nold Edu–	Nold Edu+	ADMCI Edu–	ADMCI Edu+	Statistical analysis (Edu– vs. Edu+)
N	30	30	35	35	–
Age	69.0 ± 1.2 SE	68.9 ± 1.3 SE	69.7 ± 1.1 SE	69.3 ± 1.0 SE	*T*-test: Nold-Edu– versus Nold-Edu+: 0.9 ADMCI-Edu– versus ADMCI-Edu+: 0.8
Gender (M/F)	10/20	13/17	12/23	15/20	Fisher test: Nold-Edu– versus Nold-Edu+: 0.6 ADMCI-Edu– versus ADMCI-Edu+: 0.6
Education	5.8 ± 0.3 SE	13.9 ± 0.5 SE	7.0 ± 0.2 SE	14.5 ± 0.5 SE	*T*-test: Nold-Edu– versus Nold-Edu+: $P < 0.00001$ ADMCI-Edu– versus ADMCI-Edu+: $P < 0.00001$
MMSE	28.4 ± 0.2 SE	28.4 ± 0.2 SE	25.4 ± 0.3 SE	25.2 ± 0.4 SE	Mann–Whitney *U* test: Nold-Edu– versus Nold-Edu+: 0.9 ADMCI-Edu– versus ADMCI-Edu+: 0.6

Note: MMSE, Minimental State Evaluation; M/F, males/females.

illness; (2) mixed dementia; (3) actual participation in a clinical trial using disease-modifying drugs; (4) systematic use of antidepressant drugs with anticholinergic side effects; (5) chronic use of neuroleptics, narcotics, analgesics, sedatives or hypnotics; (6) and anti-parkinsonian medications (cholinesterase inhibitors and Memantine allowed); (7) diagnosis of epilepsy or report of seizures or epileptiform EEG signatures in the past, and (8) major depression disorders described in the Diagnostic and Statistical Manual of Mental Disorders (DSM-5).

In all ADMCI patients, Apolipoprotein E (i.e., APOE) genotyping, and CSF biomarkers were assessed. CSF was preprocessed, frozen, and stored in line with the Alzheimer's Association Quality Control Programme for CSF biomarkers (Mattsson 2011). Levels of amyloid beta 1–42 (i.e., Aβ42), protein tau (i.e., total tau, t-tau), and phosphorylated form of tau (i.e., p-tau) were also measured. Furthermore, anthropometric features (i.e., weight, height, and body mass index) and cardiocirculatory markers (i.e., systolic pressure, diastolic pressure, pulse pressure, mean arterial pressure, and heart frequency) were also taken in consideration in the analysis.

Furthermore, in all ADMCI patients, the performance in various cognitive domains, including global cognitive status, memory, language, executive function, planning, visuospatial function, and attention was assessed by the following materials: (1) the global cognitive status was tested by the MMSE exam and the Alzheimer's Disease Assessment Scale-Cognitive Subscale (ADAS-Cog; Folstein et al. 1975; Rosen et al. 1984); (2) the episodic memory was assessed by the immediate and delayed recall of Rey Auditory Verbal Learning Test (Rey et al. 1968); (3) the executive functions and attention were evaluated by the Trail making test (TMT) part A and B (Reitan 1958); (4) the language was tested by 1-min verbal fluency test for letters (Novelli et al. 1986) and 1-min verbal fluency test for category (fruits, animals, or car trades; Novelli et al. 1986); and (5) planning abilities and visuospatial functions were assessed by clock drawing and copy test (Freedman et al. 1994).

Moreover, in all ADMCI patients, drugs were withdrawn for about 24 h before rsEEG recordings. This did not ensure a complete washout of the drug for obvious ethical reasons. This procedure enabled the comparison of rsEEG data while maintaining treatment in the ADMCI patients. Of note, the use of psychoactive drugs for mental disorders (i.e., sedative, anxiolytics, antidepressant, antipsychotic) and drugs for the AD treatment (e.g., acetylcholinesterase inhibitors) was controlled in all ADMCI patients. Table 3 reports all types of drugs used by ADMCI patients. Furthermore, Table 4 reports the number and the percentages of the ADMCI-Edu– and ADMCI-Edu+ patients assuming the psychoactive drugs for mental disorders before the EEG recordings. The psychoactive drugs were categorized into 2 classes. The first class included anxiety and antidepressant drugs, while the second class included antipsychotic drugs. Some ADMCI patients assumed more than one psychoactive drug. Table 4 also reports the number and the percentages of the ADMCI patients who received drugs for the AD treatment. No statistically significant difference was found between the ADMCI-Edu– and ADMCI-Edu+ groups in the use of the above medications ($P > 0.05$).

All Nold subjects underwent a cognitive screening (including MMSE and GDS) as well as physical and neurological examinations to exclude SMC, cognitive deficits, and mood disorders. All Nold subjects had a GDS score lower than the threshold of 6 (no depression) or no depression after an interview with a physician or clinical psychologist at the time of the enrolment. The Nold subjects with a history of previous or present neurological or psychiatric disease were also excluded. Furthermore, the Nold subjects affected by any chronic systemic illnesses (e.g., diabetes mellitus) were excluded, as were the Nold subjects taking chronically psychoactive drugs.

The Resting State Electroencephalographic Recordings

The rsEEG activity was recorded while the subjects were relaxed with eyes closed on a comfortable reclined chair. Instructions for rsEEG recordings encouraged the subjects to experience quiet wakefulness with muscle relaxation, no voluntary movements, no talking, and no development of systematic goal-oriented mentalization. Rather, a quiet wandering mode of mentalization was kindly required.

In all subjects, rsEEG recordings lasted about 3–5 min. The rsEEG data were recorded with a sampling frequency of

Table 3 Type of psychoactive drugs for mental disorders (i.e., sedative, anxiety, antidepressant, antipsychotic) and drugs for the AD treatment (e.g., acetylcholinesterase inhibitors, AChEIs, and *N*-methyl-d-aspartate, NMDA, receptor antagonist) received by the ADMCI patients of the present study

	ADMCI-Edu–	ADMCI-Edu+
Drugs for anxiety and depression	Daparox, Citalopram, Cimbalta, Cipralex, Entact, Lexotan, Seroplex, Sertraline, Venlafaxine, Xanax	Cimbalta, Cipralex, Efexor, Percital, Seropram, Seroplex, Trittico
Antipsychotic drugs	None	Pipamperon
Dementia drugs	Donepezil, Rivastigmine	Donepezil, Memantine

Notes: The psychoactive drugs were categorized into 2 classes: the first class includes anxiety and antidepressant drugs, while the second class includes antipsychotic drugs.

Table 4 Number and percentages of the ADMCI-Edu– ($N = 35$) and ADMCI-Edu+ ($N = 35$) patients assuming the psychoactive drugs for mental disorders (i.e., sedative, anxiety, antidepressant, antipsychotic) and drugs for the AD treatment (e.g., acetylcholinesterase inhibitors, AChEIs, and *N*-methyl-d-aspartate, NMDA, receptor antagonist) before the EEG recordings. The psychoactive drugs were categorized into 2 classes: the first class included anxiety and antidepressant drugs, while the second class included antipsychotic drugs. The results of the presence or absence of statistically significant differences (Fisher test, $P < 0.05$ corrected) between the ADMCI-Edu– and ADMCI-Edu+ subgroups as the consumption of the psychoactive and AD treatment drugs are also reported

Drugs	ADMCI-Edu–		ADMCI-Edu+		Fisher test
	N	(%)	N	(%)	
Drugs for anxiety and depression	13	37.1%	13	37.1%	$P = 1.0$
Antipsychotic drugs	0	0%	1	2.9%	$P = 1.0$
All psychoactive drugs	13	37.1%	13	37.1%	$P = 1.0$
Dementia drugs	9	25.7%	5	14.3%	$P = 0.4$
All drugs	19	54.3%	14	40%	$P = 0.8$

Notes: ADMCI-Edu– = patients with MCI due to AD and low educational level; ADMCI-Edu+ = patients with MCI due to AD and high educational level. Noteworthy, no significant difference was observed between the 2 ADMCI subgroups even when a marginal threshold of $P < 0.05$ uncorrected was used.

128–512 Hz and related antialiasing bandpass between 0.01 and 60–100 Hz. Electrode montage included 19 scalp monopolar sensors placed following 10–20 System (i.e., O1, O2, P3, Pz, P4, T3, T5, T4, T6, C3, Cz, C4, F7, F3, Fz, F4, F8, Fp1, and Fp2). A frontal ground electrode was used, while cephalic or linked earlobe electrodes were used as electric references according to local methodological facilities and standards. Electrodes impedances were kept below 5 kΩ. Vertical and horizontal electro-oculographic (EOG) potentials (0.3–70 Hz bandpass) were recorded to control eye movements and to blink.

The rsEEG Preliminary Data Analysis

The preliminary analysis of the recorded rsEEG activity followed the same procedures of previous rsEEG investigations in MCI patients of our Workgroup (Babiloni, Del Percio, Lizio, Noce, Lopez, et al. 2017a; Babiloni, Del Percio, Lizio, Noce, Cordone, et al. 2017b; Babiloni et al. 2018a, 2018b) to make comparable the results.

For this analysis, the rsEEG data were divided into epochs of 2 s and analyzed offline as follows. The rsEEG epochs affected by any physiological (ocular/blinking, muscular, and head movements) or nonphysiological (sweat, bad contact between electrodes and scalp, etc.) artifacts were identified and discarded by the visual analysis of 2 experts of EEG signals (C.D.P., G.N., S.L. or R.L.). In this visual analysis, the contamination of rsEEG rhythms with the ocular activity (i.e., blinking) was evaluated in frontal electrodes (i.e., F7, F3, Fz, F4, F8, Fp1, and Fp2), comparing EOG and EEG traces. Head movement artifacts were detected by a sudden and great increase in amplitude of slow EEG waves in all scalp electrodes. Muscle tension artifacts were recognized by observing the effects of several frequency bandpass filters in different ranges and by the inspection of rsEEG power density spectra. These artifacts were reflected by unusually high and stable values of rsEEG power density from 30 to 100 Hz, which contrast with the typical declining trend of rsEEG power density from 25 Hz onward. The experimenters also detected rsEEG epochs with signs of sleep such as K complexes, sleep spindles, vertex shape waves, and slow waves. Furthermore, the 2 experimenters carefully rejected rsEEG epochs associated with behavioral annotations taken during the experiments (e.g., drowsiness, verbal warnings, opened eyes, arm/hand movements, etc.).

As a result of the above procedures, the artifact-free epochs showed the same proportion of the total amount of rsEEG activity recorded in all groups (>85%). In particular, the mean of artifact-free rsEEG epochs were 132 (±2 SE; 88.1%) in the Nold group, 130 (±2 SE, 86.7%) in the ADMCI group, 131 (±2 SE; 87.1%) in the Nold-Edu– subgroup, 134 (±2 SE; 89.0%) in the Nold-Edu+ subgroup, 130 (±3 SE, 86.9%) in the ADMCI-Edu– subgroup, and 130 (±2 SE, 86.6%) in the ADMCI-Edu– subgroup. A statistical procedure (*T*-tests) showed no statistically significant difference ($P > 0.05$) in the amount of the artifact-free rsEEG epochs between the 2 groups (Nold vs. ADMCI: $P = 0.4$) as well as the Edu– and Edu+ subgroups (Nold-Edu– vs. Nold-Edu+: $P = 0.5$; ADMCI-Edu– vs. ADMCI-Edu+: $P = 0.9$).

The Spectral Analysis of rsEEG Epochs

A standard digital FFT-based analysis (Welch technique, Hanning windowing function, no phase shift) computed the power

density of scalp rsEEG rhythms (0.5 Hz of frequency resolution). As mentioned above, only rsEEG epochs free from artifacts were used.

The EEG frequency bands of interest were individually identified based on the following frequency landmarks, namely the transition frequency (TF) and individual alpha frequency peak (IAFp; Klimesch 1999). In the EEG power density spectrum, the TF marks the transition frequency between the theta and alpha bands, defined as the minimum of the rsEEG power density between 3 and 8 Hz (between the delta and the alpha power peak). The IAF is defined as the maximum power density peak between 6 and 14 Hz. These frequency landmarks were previously well described by Dr Wolfgang Klimesch (Klimesch et al. 1996, 1998; Klimesch 1999).

The TF and IAF were computed for each subject involved in the study. Based on the TF and IAF, we estimated the individual delta, theta, and alpha bands as follows: delta from TF –4 Hz to TF –2 Hz, theta from TF –2 Hz to TF, low-frequency alpha (alpha 1 and alpha 2) from TF to IAF, and high-frequency alpha (or alpha 3) from IAF to IAF + 2 Hz. Specifically, the individual alpha 1 and alpha 2 bands were computed as follows: alpha 1 from TF to the frequency midpoint of the TF–IAF range and alpha 2 from that midpoint to IAF. The other bands were defined based on the standard fixed frequency ranges used in the reference study (Babiloni, Del Percio, Lizio, Noce, Lopez, et al. 2017a; Babiloni, Del Percio, Lizio, Noce, Cordone, et al. 2017b): beta 1 from 14 to 20 Hz, beta 2 from 20 to 30 Hz, and gamma from 30 to 40 Hz.

Of note, important aspects of the procedure were the following: (1) we divided the alpha band into sub-bands because, in the eyes-closed rsEEG condition, dominant low-frequency alpha rhythms (alpha 1 and alpha 2) may denote the synchronization of diffuse neural networks regulating the fluctuation of the subject's global awake and conscious states, while high-frequency alpha rhythms (alpha 3) may denote the synchronization of more selective neural networks specialized in the processing of modal specific or semantic information (Klimesch 1999; Pfurtscheller and Lopes da Silva 1999). When the subject is engaged in sensorimotor or cognitive tasks, alpha and low-frequency beta (beta 1) rhythms reduce in power (i.e., desynchronization or blocking) and are replaced by fast EEG oscillations at high-frequency beta (beta 2) and gamma rhythms (Pfurtscheller and Lopes da Silva 1999); (2) we considered individual delta, theta, and alpha frequency bands because of a clinical group may be characterized by a mean slowing in the peak frequency of the alpha power density without any substantial change in the magnitude of the power density. In that specific case, the use of fixed frequency bands would result in a statistical effect erroneously showing alpha power density values lower in the clinical than the control group; (3) we used fixed frequency ranges for the beta and gamma bands because of the individual beta and gamma frequency peaks were evident only in a few subjects (<10%); (4) we selected the beginning of the beta frequency range at 14 Hz to avoid the overlapping between individual alpha and fixed beta frequency ranges (i.e., individual alpha frequency band ranged from TF to 14 Hz with an IAF = 12 Hz).

The Estimation of rsEEG Cortical Sources by eLORETA Freeware

We used the official freeware tool called exact low-resolution brain electromagnetic tomography (eLORETA) for the linear estimation of the cortical source activation generating scalp-recorded rsEEG rhythms (Pascual-Marqui 2007). The present implementation of eLORETA uses a spherical head volume conductor model composed of the scalp, skull, and brain. In the scalp compartment, exploring electrodes can be virtually positioned to give EEG data as an input to the source estimation (Pascual-Marqui 2007). The brain model is based on a realistic cerebral shape taken from a template typically used in the neuroimaging studies, namely that of the Montreal Neurological Institute (MNI152 template). The eLORETA freeware solves the so-called EEG inverse problem estimating "neural" current density values at any cortical voxel of the mentioned spherical head volume conductor model. The solutions are computed at all rsEEG frequency bin-by-frequency bin (0.5 Hz as frequency resolution, namely, the maximum frequency resolution allowed by the use of 2-s artifact-free EEG epochs).

The input for eLORETA source estimation is the set of artifact-free EEG epochs with 19 scalp electrodes, placed according to the 10–20 montage system. The output is the set of estimates of neural ionic currents in the brain source space formed by 6239 voxels with 5 mm resolution, restricted to the cortical gray matter of the spherical head volume conductor model. In that cortical source space, an equivalent current dipole is located in each voxel. For each voxel, the eLORETA package provides the Talairach coordinates, the cortical lobe, and the Brodmann area (BA).

In line with the general low spatial resolution of the present EEG methodological approach (i.e., 19 scalp electrodes), we performed a regional analysis of the eLORETA solutions. The following 6 lobar macroregions of interest (ROIs) were considered: frontal (Brodmann area, BA 8, 9, 10, 11, 44, 45, 46, and 47), central (BA 1, 2, 3, 4, and 6), parietal (BA 5, 7, 30, 39, 40, and 43), occipital (BA 17, 18, and 19), temporal (BA 20, 21, 22, 37, 38, 41, and 42), and limbic (BA 31, 32, 33, 34, 35, 36). Remarkably, the eLORETA solution for each lobar ROI was obtained by the average of the normalized eLORETA current density values estimated at all single voxels included in that ROI. For example, the eLORETA solution for the temporal ROI was obtained by the average of the normalized eLORETA current density values estimated at all voxels included in the BA 20, 21, 22, 37, 38, 41, and 42 of the bilateral temporal lobes. Similarly, the eLORETA solution for the occipital ROI was obtained by the same principle for the BA 17, 18, and 19 of the bilateral occipital lobes.

Statistical Analysis of the rsEEG Source Activity

Three statistical sessions were performed by the commercial tool STATISTICA 10 (StatSoft Inc., www.statsoft.com) to test the study hypotheses. In all statistical sessions, an ANOVA was computed using the rsEEG source activations (i.e., regional normalized eLORETA solutions) as a dependent variable ($P < 0.05$). It is well-known that the use of ANOVA models implies that dependent variables approximate Gaussian distributions, so we tested this feature in the eLORETA solutions by Kolmogorov–Smirnov test (null hypothesis of non-Gaussian distributions tested at $P > 0.05$). As the distributions of the eLORETA solutions were not Gaussian in all cases, those solutions underwent to the log-10 transformation and retested. Such a transformation is a popular method to transform skewed data distribution with all positive values (as eLORETA solutions are) to Gaussian distributions, thus augmenting the reliability of the ANOVA results. Indeed, the outcome of the procedure approximated the distributions of all eLORETA solutions to Gaussian distributions ($P > 0.05$), allowing the use of the ANOVA model.

Mauchly's test evaluated the sphericity assumption, and degrees of freedom were corrected by the Greenhouse–Geisser procedure when appropriate ($P < 0.05$). Duncan test was used for posthoc comparisons ($P < 0.05$, corrected for multiple comparisons).

The results of the following statistical analyses were controlled by the iterative (leave-one-out) Grubbs' test detecting for the presence of one or more outliers in the distribution of the eLORETA source solutions. The null hypothesis of the nonoutlier status was tested at the arbitrary threshold of $P > 0.001$ to remove only individual values with high probability to be outliers.

The first ANOVA tested the hypothesis that the rsEEG source activities (i.e., regional normalized eLORETA solutions) at alpha frequencies were abnormal in the ADMCI patients as compared to the Nold seniors. The ANOVA factors were Group (Nold and ADMCI), Band (delta, theta, alpha 1, alpha 2, alpha 3, beta 1, beta 2, and gamma), and ROI (frontal, central, parietal, occipital, temporal, and limbic). The confirmation of the hypothesis would require: (1) a statistically significant ANOVA interaction including the factors Group and Band ($P < 0.05$) and (2) a posthoc Duncan test indicating statistically significant ($P < 0.05$ Bonferroni corrected) differences in the rsEEG source activities at alpha frequencies between the Nold and ADMCI groups (i.e., Nold $\neq$ ADMCI, $P < 0.05$ Bonferroni corrected).

The second ANOVA evaluated the hypothesis that the rsEEG source activities at alpha frequencies (i.e., regional normalized eLORETA solutions) were related to the educational attainment in the Nold seniors (Nold-Edu− vs. Nold-Edu+). The ANOVA factors were Subgroup (Nold-Edu− and Nold-Edu+), Band (delta, theta, alpha 1, alpha 2, alpha 3, beta 1, beta 2, and gamma), and ROI (frontal, central, parietal, occipital, temporal, and limbic). The confirmation of the hypothesis would require: (1) a statistically significant ANOVA interaction including the factors Subgroup and Band ($P < 0.05$) and (2) a posthoc Duncan test indicating statistically significant ($P < 0.05$ Bonferroni corrected) differences in the rsEEG source activities at alpha frequencies between the Nold-Edu− and Nold-Edu+ subgroups (i.e., Nold-Edu− $\neq$ Nold-Edu+, $P < 0.05$ Bonferroni corrected).

The third ANOVA evaluated the hypothesis that the rsEEG source activities at alpha frequencies (i.e., regional normalized eLORETA solutions) were related to the educational attainment in the ADMCI patients (ADMCI-Edu− vs. ADMCI-Edu+). The ANOVA factors were Subgroup (ADMCI-Edu− and ADMCI-Edu+), Band (delta, theta, alpha 1, alpha 2, alpha 3, beta 1, beta 2, and gamma), and ROI (frontal, central, parietal, occipital, temporal, and limbic). The confirmation of the hypothesis may require: (1) a statistically significant ANOVA interaction including the factors Subgroup and Band ($P < 0.05$) and (2) a posthoc Duncan test indicating statistically significant ($P < 0.05$ Bonferroni corrected) differences in the rsEEG source activities at alpha frequencies between the ADMCI-Edu− and ADMCI-Edu+ subgroups (i.e., ADMCI-Edu− $\neq$ ADMCI-Edu+, $P < 0.05$ Bonferroni corrected).

Results

Control Markers in the Patients with Alzheimer's Disease Mild Cognitive Impairment Having Low (Edu−) and High (Edu+) Education Attainment

Table 5 reports the most relevant clinical (i.e., GDS, CDR, and Hachinski Ischemic Score, HIS), genetic (i.e., APOE genotyping), and CSF (i.e., Aβ42, t-tau, p-tau; Aβ42/p-tau) features of the ADMCI-Edu− and ADMCI-Edu+ subgroups. Table 5 also reports the results of the presence or absence of statistically significant differences ($P < 0.05$) between the 2 subgroups (i.e., ADMCI-Edu− and ADMCI-Edu+) for the above mentioned clinical (*T*-test), genetic (Fisher test), and CSF (*T*-test) markers. To consider the inflating effects of repetitive univariate tests, the statistical threshold was set at $P < 0.00625$ (i.e., 8 markers, $P < 0.05/8 = 0.00625$) to obtain the Bonferroni correction at $P < 0.05$. Statistically significant differences were found neither considering that correction ($P > 0.05$ uncorrected) nor ignoring that correction ($P > 0.05$).

Table 6 reports the mean values (±SE) of the following neuropsychological tests in the ADMCI-Edu− and ADMCI-Edu+ subgroups: ADAS-Cog, Rey Auditory Verbal Learning Test (immediate and delayed recall), TMT B-A, Verbal fluency for letters, Verbal fluency for category, Clock drawing, and Clock copy. Table 6 also includes the cut-off scores of above-mentioned neuropsychological tests (Novelli et al. 1986; Watson et al. 1993; Caltagirone et al. 1995; Giovagnoli et al. 1996; Monllau et al. 2007) and the results of the presence or absence of statistically significant differences (*T*-test; log-10 transformed data) between the 2 subgroups (i.e., ADMCI-Edu− and ADMCI-Edu+) for the neuropsychological tests used. To consider the inflating effects of repetitive univariate tests, the statistical threshold was set at $P < 0.00625$ (i.e., 8 neuropsychological tests, $P < 0.05/8 = 0.00625$) to obtain the Bonferroni correction at $P < 0.05$. A statistically significant difference was only found for the TMT B-A score ($P < 0.008$), unveiling a worsening of TMT B-A score in the ADMCI-Edu− as compared to the ADMCI-Edu+ subgroup. Furthermore, a worsening of the Rey Auditory Verbal Learning Test (delayed recall; $P = 0.01$), Clock drawing ($P = 0.01$), and Clock copy scores ($P = 0.01$) was found in the ADMCI-Edu+ as compared to the ADMCI-Edu− subgroup using an explorative statistical threshold of $P < 0.05$ uncorrected.

RsEEG Source Activities in the Normal Old (Nold) Versus ADMCI Subgroups

Table 7 (top) reports the mean values of TF and IAF for the Nold and ADMCI groups, together with the results of the statistical comparisons between them (*T*-test). The statistical threshold was set at $P < 0.025$ (i.e., 2 markers, $P < 0.05/2 = 0.025$) to obtain the Bonferroni correction at $P < 0.05$. The mean TF was of 6.0 Hz (±0.2 SE) in the Nold group and 5.4 Hz (±0.2 SE) in the ADMCI group. Furthermore, the mean IAF was of 9.3 Hz (±0.2 SE) in the Nold group and 8.5 Hz (±0.2 SE) in the ADMCI group. The *T*-tests showed that the mean TF ($P < 0.005$) and IAF ($P < 0.001$) values were lower in the ADMCI than the Nold group. These findings emphasized the importance of the use of the TF and IAF in the determination of the delta to alpha frequency bands in the studies involving ADMCI patients.

Figure 1 shows the mean values (±SE, log-10 transformed) of regional rsEEG source activations (i.e., normalized eLORETA solutions) relative to a statistically significant ANOVA interaction effect ($F = 15.3$; $P < 0.0001$) among the factors Group (Nold and ADMCI), Band (delta, theta, alpha 1, alpha 2, alpha 3, beta 1, beta 2, and gamma), and ROI (frontal, central, parietal, occipital, temporal, and limbic). In the Nold group, the eLORETA solutions showed maximum magnitude in the occipital (maximum), parietal, temporal, and limbic alpha 2 and alpha 3 sources. Compared to the Nold group, the ADMCI group showed a substantial decrease in the eLORETA solutions in posterior (i.e., central,

Table 5 Mean values (±SE) of the clinical (i.e., GDS, CDR, and Hachinski Ischemic Score), genetic (i.e., Apolipoprotein E genotyping, APOE), and CSF (i.e., beta amyloid 1–42, Aβ 42; protein tau, t-tau; and phosphorylated form of protein tau, p-tau) data as the results of their statistical comparisons ($P < 0.05$) in the subgroups of ADMCI-Edu– ($N = 35$) and ADMCI-Edu+ ($N = 35$) patients. In line with the inclusion criteria, all ADMCI patients had CDR score of 0.5, GDS score ≤ 5, and HIS score ≤ 4

Clinical, genetic (APOE) and CSF markers in ADMCI-Edu– and ADMCI-Edu+			
	ADMCI-Edu–	ADMCI-Edu+	Statistical analyses
Clinical markers			
Geriatric depression scale (GDS)	2.6 ± 0.3	2.6 ± 0.3	*T*-test: $P = 1.0$
Clinical dementia rating (CDR)	0.5 ± 0.0	0.5 ± 0.0	*T*-test: $P = 1.0$
Hachinski ischemic score (HIS)	0.8 ± 0.1	0.8 ± 0.1	*T*-test: $P = 1.0$
Genetic marker			
APOE4 (%)	78.6%	84.9%	Fisher test: $P = 0.8$
Cerebrospinal fluid markers			
Aβ42 (pg/mL)	505 ± 25	492 ± 22	*T*-test: $P = 0.9$
p-tau (pg/mL)	89 ± 7	82 ± 6	*T*-test: $P = 0.6$
t-tau (pg/mL)	605 ± 62	653 ± 78	*T*-test: $P = 0.5$
Aβ42/p-tau	7.0 ± 0.6	6.8 ± 0.5	*T*-test: $P = 0.9$

Notes: ADMCI-Edu– = patients with MCI due to AD and low educational level; ADMCI-Edu+ = patients with MCI due to AD and high educational level. Noteworthy, no significant difference was observed between the 2 ADMCI groups even when a marginal threshold of $P < 0.05$ uncorrected was used

Table 6 Mean values (±SE) of the neuropsychological scores (i.e., ADAS-Cog, Rey Auditory Verbal Learning Test immediate recall, Rey Auditory Verbal Learning Test delayed recall, TMT part B-A, Verbal fluency for letters, Verbal fluency for category, Clock drawing, and Clock copy) as well as the results of their statistical comparisons (*T*-test on log-10 transformed data; $P < 0.05$ corrected) in the subgroups of ADMCI-Edu– ($N = 35$) and ADMCI-Edu+ ($N = 35$) patients. The cut-off scores of the neuropsychological tests are also reported

Neuropsychological markers in ADMCI-Edu– and ADMCI-Edu+				
	Cut-off of abnormality	ADMCI-Edu– Mean ± SE (% subjects with abnormal score)	ADMCI-Edu+ Mean ± SE (% subjects with abnormal score)	*T*-test
ADAS-Cog	≥17	22.7 ± 1.3 (76%)	20.4 ± 1.1 (70%)	$P = 0.4$
RAVLT immediate recall	<28.53	28.3 ± 1.5 (51%)	28.9 ± 1.7 (49%)	$P = 0.9$
RAVLT delayed recall	<4.69	4.3 ± 0.5 (60%)	2.9 ± 0.5 (83%)	$P = 0.01$
Trail Making test B-A	≥187	164.3 ± 10.8 (42%)	110.9 ± 11.2 (14%)	$P = 0.0004$
Clock drawing	>3	3.4 ± 0.2 (52%)	4.2 ± 0.3 (81%)	$P = 0.01$
Clock copy	>3	4.2 ± 0.2 (80%)	4.8 ± 0.1 (97%)	$P = 0.01$
Letter fluency	<17	30.3 ± 2.0 (11%)	35.3 ± 1.9 (6%)	$P = 0.1$
Letter category	<25	28.8 ± 1.9 (36%)	35.5 ± 2.2 (26%)	$P = 0.1$

Notes: ADMCI-Edu– = patients with MCI due to AD and low educational level; ADMCI-Edu+ = patients with MCI due to AD and high educational level; ADAS-Cog = Alzheimer's Disease Assessment Scale-Cognitive Subscale; RAVLT = Rey Auditory Verbal Learning Test; TMT B-A = Trail Making Test part B-A. Noteworthy, a statistically significant difference ($P < 0.05$ corrected) was observed between the 2 ADMCI groups for the TMT B-A score. Namely, the TMT B-A score was worse in the ADMCI-Edu– than the ADMCI-Edu+ subgroup ($P = 0.0004$). Furthermore, a marginal difference was observed between the 2 ADMCI subgroups when a marginal threshold of $P < 0.05$ uncorrected was used. Namely, the RAVLT delayed recall, Clock drawing, and Clock copy score was worse in the ADMCI-Edu+ than the ADMCI-Edu– subgroup ($P = 0.01$ uncorrected).

parietal, occipital, and temporal) alpha 2 and alpha 3 sources. Furthermore, the ADMCI group showed a substantial increase in the eLORETA solutions in widespread delta sources.

The Duncan planned posthoc ($P < 0.05$ Bonferroni correction for 8 frequency bands ×6 ROIs = 48, $P < 0.05/48 = 0.001$) testing showed that: (1) the discriminant pattern Nold > ADMCI was fitted by central ($P = 0.000001$), parietal ($P = 0.000005$), occipital ($P = 0.000001$), temporal ($P = 0.000001$), and limbic ($P = 0.000005$) alpha 2 source activities as well as central ($P = 0.000001$), parietal ($P = 0.000005$), occipital ($P = 0.000005$), temporal ($P = 0.000005$), and limbic ($P = 0.000001$) alpha 3 source activations; (2) the discriminant pattern Nold < ADMCI was fitted by the frontal ($P = 0.00005$), central ($P = 0.0005$), parietal ($P = 0.000005$), and temporal ($P = 0.000005$) delta source activations. Of note, these findings were not due to outliers from those individual eLORETA solutions (log-10 transformed), as shown by Grubbs' test with an arbitrary threshold of $P > 0.001$ (see Fig. 2).

RsEEG Source Activities in the Nold-Edu− versus Nold-Edu+ Subgroups

Table 7 (bottom) reports the mean values of TF and IAF for the Nold-Edu– and Nold-Edu+ subgroups, together with the results of the statistical comparisons between them (*T*-test). The statistical threshold was set at $P < 0.025$ (i.e., 2 markers, $P < 0.05/2 = 0.025$) to obtain the Bonferroni correction at $P < 0.05$. The mean TF was of 6.0 Hz (±0.1 SE) in the Nold-Edu– subgroup and 5.9 Hz (±0.2 SE) in the Nold-Edu+ subgroup. Furthermore, the mean IAF was of 9.4 Hz (±0.1 SE) in the Nold-Edu– subgroup and 9.1 Hz (±0.1 SE) in the Nold-Edu+ subgroup. Statistically significant differences were found neither considering that correction (*T*-test, $P > 0.05$ uncorrected) nor ignoring that correction ($P > 0.05$).

Figure 3 shows the mean values (±SE, log-10 transformed) of global rsEEG source activations (i.e., normalized eLORETA

Table 7 (Top): Mean values (±SE) of TF and IAF peak computed from resting state EEG (rsEEG) power density spectra in the Nold ($N = 60$) and ADMCI ($N = 70$) groups. The results of the presence or absence of statistically significant differences (T test, $P < 0.05$ corrected) between the Nold and ADMCI groups are also reported; (Bottom): Mean values (±SE) of TF and IAF computed from rsEEG power density spectra in the Nold-Edu– ($N = 30$), Nold-Edu+ ($N = 30$), ADMCI-Edu– ($N = 35$), and ADMCI-Edu+ ($N = 35$) subgroups. The results of the presence or absence of statistically significant differences (T test, $P < 0.05$ corrected) between the 2 Nold (Nold-Edu– vs. Nold Edu+) and ADMCI (ADMCI-Edu– vs. ADMCI-Edu+) subgroups are also reported

TF and IAF peak					
	Nold		**ADMCI**		**T test (Nold vs. ADMCI)**
TF	6.0 ± 0.2 SE		5.4 ± 0.1 SE		*T*-test: **$P < 0.005$**
IAF	9.3 ± 0.2 SE		8.5 ± 0.2 SE		*T*-test: **$P < 0.001$**
	Nold Edu–	**Nold Edu+**	**ADMCI Edu–**	**ADMCI Edu+**	**T test (Edu– vs. Edu+)**
TF	6.0 ± 0.2 SE	5.9 ± 0.1 SE	5.3 ± 0.2 SE	5.5 ± 0.2 SE	Nold-Edu– versus Nold-Edu+: $P = 0.7$ ADMCI-Edu– versus ADMCI-Edu+: $P = 0.3$
IAF	9.4 ± 0.1 SE	9.1 ± 0.1 SE	8.4 ± 0.3 SE	8.5 ± 0.3 SE	Nold-Edu– vs. Nold-Edu+: $P = 0.2$ ADMCI-Edu– vs. ADMCI-Edu+: $P = 0.7$

Notes: Nold-Edu– = healthy elderly subjects with low educational level; Nold-Edu+ = healthy elderly subjects with high educational level; ADMCI-Edu– = patients with MCI due to AD and low educational level; ADMCI-Edu+ = patients with MCI due to AD and high educational level

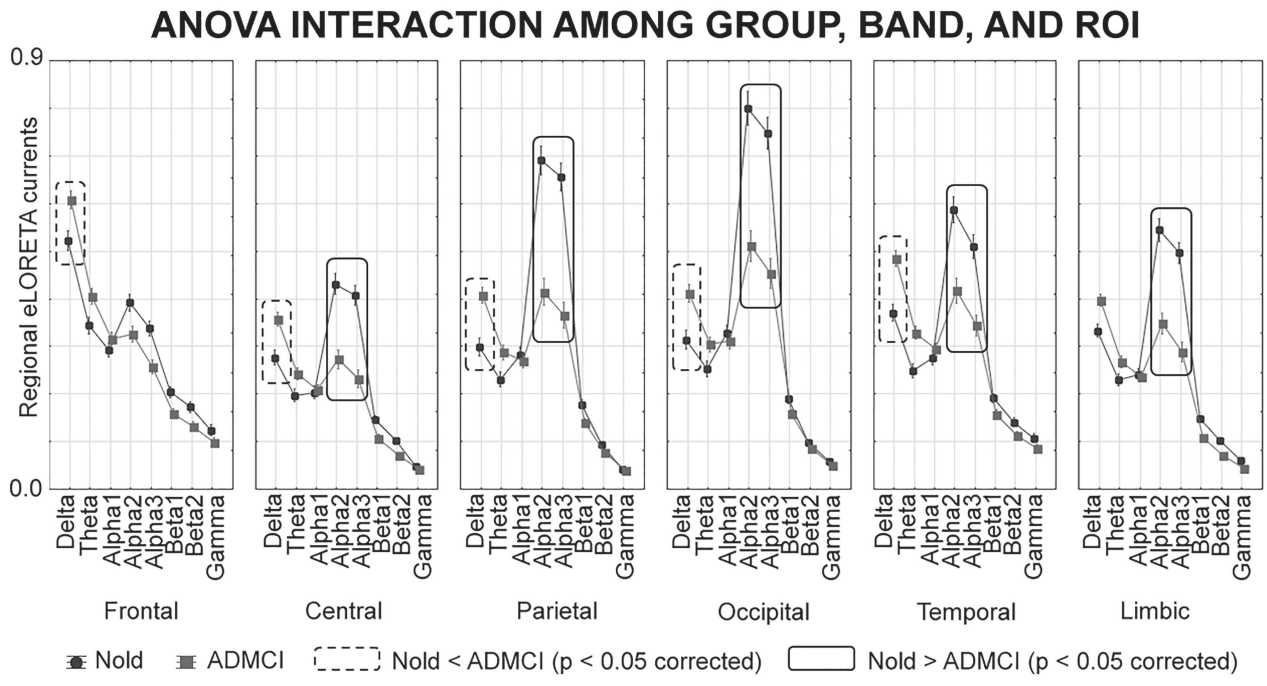

Figure 1. Regional normalized exact low-resolution brain electromagnetic source tomography (eLORETA) solutions (mean across subjects, log-10 transformed) modeling cortical sources of eyes-closed rsEEG rhythms relative to a statistical ANOVA interaction ($F = 15.3$, $P < 0.0001$) among the factors Group (Nold, $N = 60$; ADMCI, $N = 70$), Band (delta, theta, alpha 1, alpha 2, alpha 3, beta 1, beta 2, and gamma), and ROI (central, frontal, parietal, occipital, temporal, and limbic). This ANOVA design used the regional normalized eLORETA solutions as a dependent variable. Regional normalized eLORETA solutions modeled the rsEEG relative power spectra as revealed by a sort of "virtual" intracranial macroelectrodes located on the macrocortical regions of interest. Notes: The rectangles indicate the cortical regions and frequency bands in which the eLORETA solutions statistically presented a significant eLORETA pattern Nold ≠ ADMCI ($P < 0.05$ corrected = $P < 0.001$).

solutions) relative to a statistically significant ANOVA interaction effect ($F = 5.5$; $P < 0.0001$) between the factors Subgroup (Nold-Edu– and Nold-Edu+) and Band (delta, theta, alpha 1, alpha 2, alpha 3, beta 1, b eta 2, and gamma). The Duncan planned posthoc testing ($P < 0.05$ Bonferroni correction for 8 frequency bands, $P < 0.05/8 = 0.00625$) disclosed that the discriminant pattern Nold-Edu+ > Nold-Edu– was fitted by the global alpha 2 ($P = 0.00001$) and alpha 3 ($P = 0.0001$) source activations across all ROIs ($P = 0.001$). Namely, the global alpha 2 and alpha 3 source activations were greater in the Nold-Edu+ than the Nold-Edu subgroup. Of note, those findings were not due to outliers from those individual eLORETA solutions (log-10 transformed), as shown by Grubbs' test with an arbitrary threshold of $P > 0.001$ (see Fig. 4).

The effect sizes (Cohen's *d*) and sample size were calculated for the relevant global alpha 2 and alpha 3 source activations with alpha level of 0.05 one-tail and a power of 80%. The effect sizes were –0.80 for the global alpha 2 source activity and –0.64 for the global alpha 3 source activity. The sample sizes were 21 Nold subjects (for each subgroup) for the global alpha 2 source activity and 31 Nold subjects for the global alpha 3 source activity.

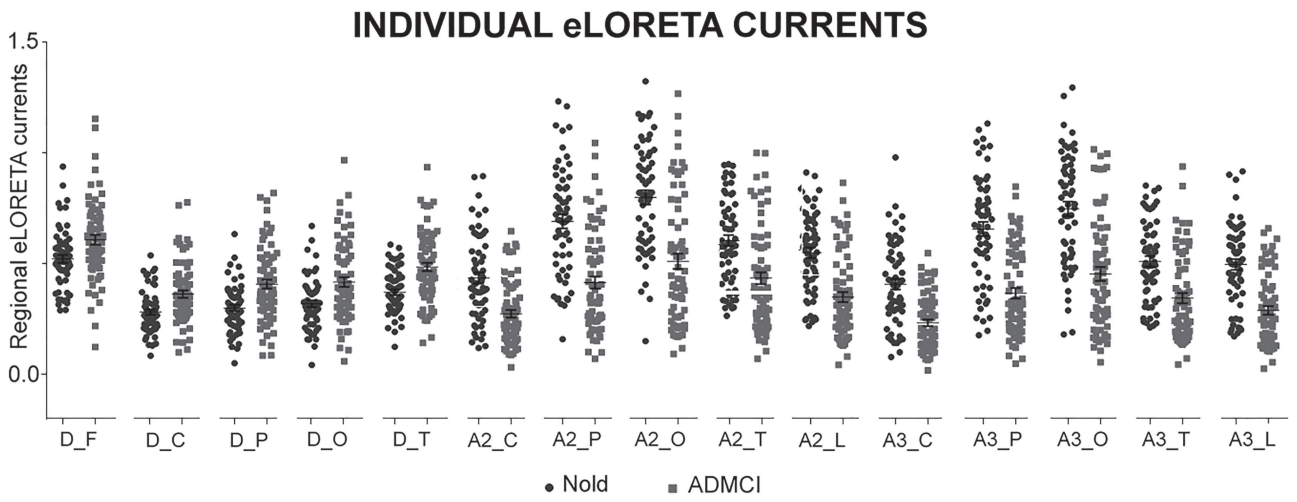

Figure 2. Individual values (log-10 transformed) of the regional normalized eLORETA solutions (i.e., D_F: frontal delta; D_C: central delta; D_P: parietal delta; D_O: occipital delta; D_T: temporal delta; A2_C: central alpha 2; A2_P: parietal alpha 2; A2_O: occipital alpha 2; A2_T: temporal alpha 2; A2_L: limbic alpha 2; A3_C: central alpha 3; A3_P: parietal alpha 3; A3_O: occipital alpha 3; A3_T: temporal alpha 3; A3_L: limbic alpha 3) showing statistically significant ($P < 0.001$ to have a $P < 0.05$ corrected for multiple post-hoc comparisons) differences between Nold ($N = 60$) and ADMCI ($N = 70$) groups. Noteworthy, the Grubbs' test showed no outliers from those individual values of the eLORETA solutions (arbitrary threshold of $P < 0.001$).

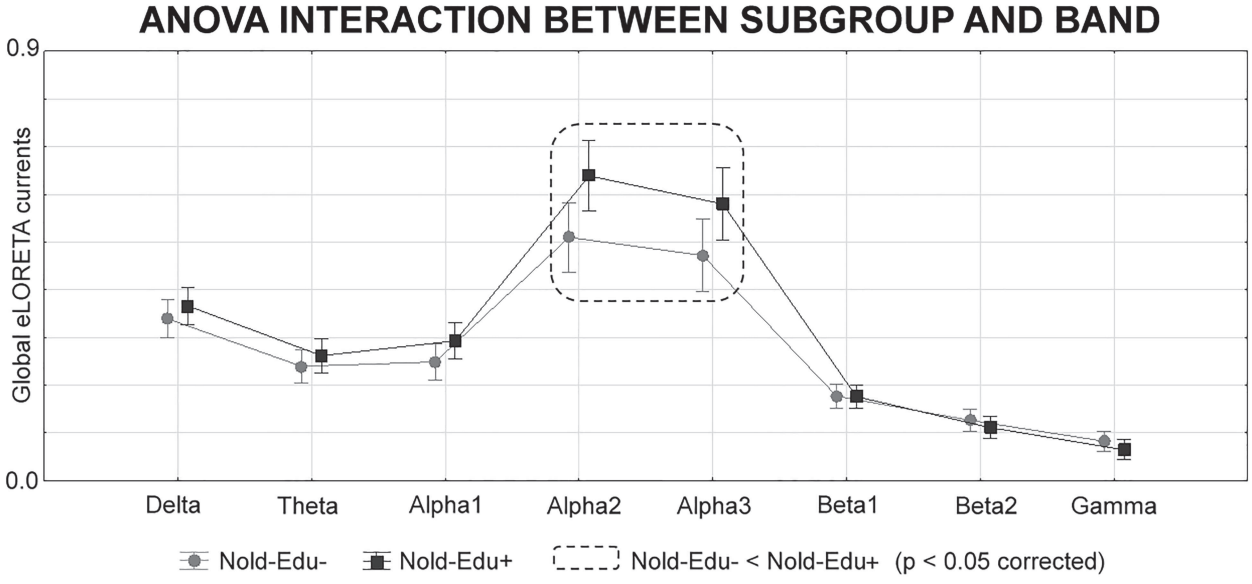

Figure 3. Normalized eLORETA solutions (mean across subjects, log-10 transformed) modeling cortical sources of eyes-closed rsEEG rhythms relative to a statistical ANOVA interaction ($F = 5.5$, $P < 0.0001$) among the factors Subgroup (healthy elderly subjects with low educational level, Nold-Edu–, $N = 30$; healthy elderly subjects with high educational level, Nold-Edu+, $N = 30$) and Band (delta, theta, alpha 1, alpha 2, alpha 3, beta 1, beta 2, and gamma). This ANOVA design used the regional normalized eLORETA solutions as a dependent variable. Notes: The rectangles indicate the frequency bands in which the eLORETA solutions statistically presented a significant eLORETA pattern Nold-Edu– ≠ ADMCI-Nold+ ($P < 0.05$ corrected = $P < 0.00625$).

RsEEG Source Activities in the ADMCI-Edu– Versus ADMCI-Edu+ Subgroups

Table 7 (bottom) reports the mean values of TF and IAF for the ADMCI-Edu– and ADMCI-Edu+ subgroups, together with the results of the statistical comparisons between them (*T*-test). The statistical threshold was set at $P < 0.025$ (i.e., 2 markers, $P < 0.05/2 = 0.025$) to obtain the Bonferroni correction at $P < 0.05$. The mean TF was of 5.3 Hz (±0.2 SE) in the ADMCI-Edu– subgroup and 5.5 Hz (±0.2 SE) in the ADMCI-Edu+ subgroup. Furthermore, the mean IAF was of 8.4 Hz (±0.2 SE) in the ADMCI-Edu– subgroup and 8.5 Hz (±0.2 SE) in the ADMCI-Edu+ subgroup. Statistically significant differences were found neither considering that correction (*T*-test, $P > 0.05$ uncorrected) nor ignoring that correction ($P > 0.05$).

Figure 5 shows the mean values (±SE, log-10 transformed) of global rsEEG source activations (i.e., normalized eLORETA solutions) relative to a statistically significant ANOVA interaction effect ($F = 2.1$; $P < 0.05$) between the factors Subgroup (ADMCI-Edu– and ADMCI-Edu+) and Band (delta, theta, alpha 1, alpha 2, alpha 3, beta 1, beta 2, and gamma). The Duncan planned posthoc testing ($P < 0.05$ Bonferroni correction for 8 frequency bands, $P < 0.05/8 = 0.00625$) showed that the discriminant

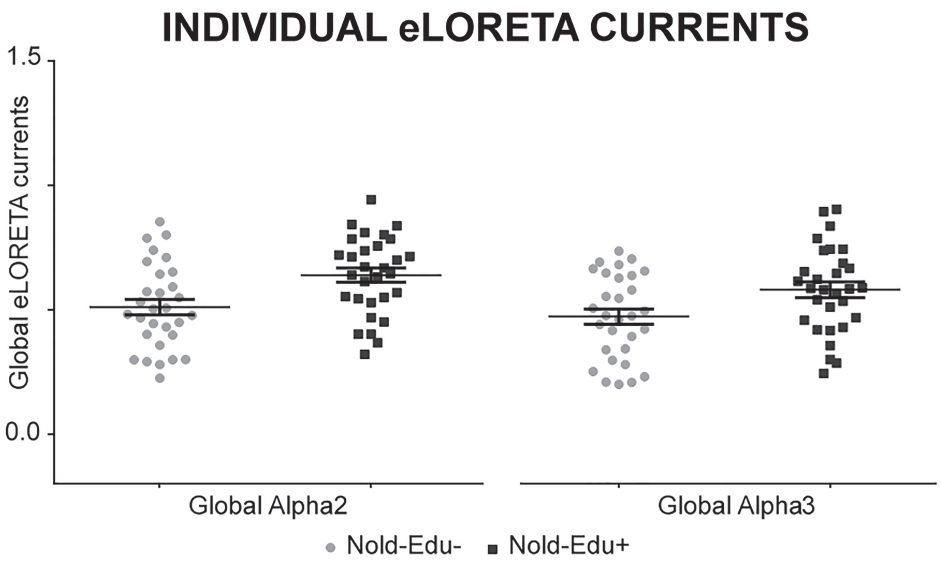

Figure 4. Individual values (log-10 transformed) of the global alpha 2 and alpha 3 normalized eLORETA solution showing statistically significant ($P < 0.00625$ to have a $P < 0.05$ corrected for multiple post-hoc comparisons) difference between Nold-Edu– ($N = 30$) and Nold-Edu+ ($N = 30$) subgroups. Noteworthy, the Grubbs' test showed no outliers from those individual values of the eLORETA solutions (arbitrary threshold of $P < 0.001$).

pattern ADMCI-Edu+ < ADMCI-Edu– was fitted by global alpha 2 ($P = 0.005$) and alpha 3 ($P = 0.001$) source activations. Namely, the global alpha 2 and 3 source activations were lower in the ADMCI-Edu+ than the ADMCI-Edu subgroup. Of note, those finding were not due to outliers from those individual eLORETA solutions (log-10 transformed), as shown by Grubbs' test with an arbitrary threshold of $P > 0.001$ (see Fig. 6).

The effect sizes (Cohen's *d*) and sample size were calculated for the relevant global alpha 2 and alpha 3 source activations. The effect sizes were 0.49 for the global alpha 2 source activity and 0.65 for the global alpha 3 source activity. The sample sizes were 53 ADMCI patients (for each subgroup) for the global alpha 2 source activity and 30 ADMCI patients for the global alpha 3 source activity.

Results of the Control Analyses

A control analysis was performed to confirm that the above rsEEG (eLORETA) source differences between the ADMCI-Edu– and ADMCI-Edu+ subgroups may be not due to (1) the global neurodegeneration of the cerebral cortex; (2) the neurodegeneration of cerebral structures as the mesial temporal cortex, basal ganglia, and lateral ventricle; and (3) cerebrovascular lesions. In that control analysis, we evaluated whether the MRI markers may differ between the ADMCI-Edu– and ADMCI-Edu+ subgroups. For each ADMCI patient, the procedure was as follows: (1) the MRI markers included: (i) the total gray matter (GM) and white matter (WM) volumes (normalized respect to total intracranial volume) and the total cortical thickness; (ii) the volumes of caudate, putamen, pallidum, accumbens, hippocampus, amygdala, and lateral ventricle (normalized with respect to total intracranial volume), and the cortical thicknesses of entorhinal cortex; and (iii) the WM hypointensity and WM lesions; (2) the MRI markers were log-10 transformed to make them Gaussian before the subsequent parametric statistical analysis; (3) *T*-tests were computed to evaluate the presence or absence of statistically significant differences between the 2 ADMCI groups for the above-mentioned MRI markers. To consider the inflating effects of repetitive univariate tests, the statistical threshold was set at $P < 0.0038$ (i.e., 13 MRI markers, $P < 0.05/13 = 0.0038$) to obtain the Bonferroni correction at $P < 0.05$. Statistically significant differences were found neither considering that correction ($P > 0.05$ uncorrected) nor ignoring that correction ($P > 0.05$; see Table 8).

Overall, the above control analysis confirmed that the rsEEG (eLORETA) source differences between the ADMCI-Edu– and ADMCI-Edu+ groups were not merely due to the neurodegeneration of cortical structures or cerebrovascular lesions.

Discussion

The present study aimed at testing whether, as compared to the low CR, the high CR (proxy: education attainment) may be associated with (1) greater rsEEG alpha source activations in the Nold seniors as a potential neuroprotective mechanism and (2) reduced alpha source activations in the ADMCI patients subtending a potential compensatory mechanism mitigating the impact of that reduction on patients' cognitive status.

Cognitive Reserve and rsEEG Alpha Rhythms in the Nold Seniors

Here we report that the Nold-Edu+ subgroup (higher education attainment) showed greater alpha source activations topographically widespread as compared to the Nold-Edu– subgroup (lower education attainment). In contrast, the other rsEEG frequency bands including delta and theta exhibited no significant effects in relationship to the CR.

These findings extend previous rsEEG evidence obtained in young and Nold adults revealing that a high CR was related to an enhanced functional coupling of alpha rhythms topographically widespread (Fleck et al. 2017, 2019). Furthermore, they extend previous rsEEG evidence found in SMC seniors negative to Alzheimer's amyloid- biomarkers; namely, those SMC-Edu+

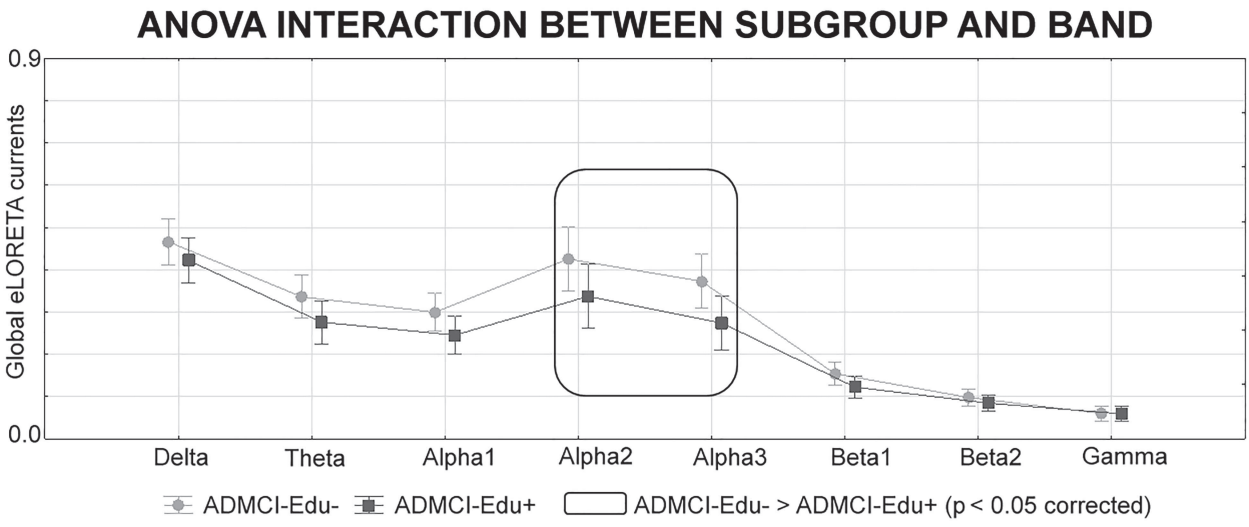

Figure 5. Normalized eLORETA solutions (mean across subjects, log-10 transformed) modeling cortical sources of eyes-closed rsEEG rhythms relative to a statistical ANOVA interaction ($F = 2.1$, $P < 0.05$) among the factors Subgroup (patients with mild cognitive due to AD and low educational level, ADMCI-Edu–, $N = 35$; patients with mild cognitive due to AD and high educational level, ADMCI-Edu+, $N = 35$) and Band (delta, theta, alpha 1, alpha 2, alpha 3, beta 1, beta 2, and gamma). This ANOVA design used the regional normalized eLORETA solutions as a dependent variable. Notes: The rectangles indicate the frequency bands in which the eLORETA solutions statistically presented a significant eLORETA pattern ADMCI-Edu– ≠ ADMCI-Edu+ ($P < 0.05$ corrected = $P < 0.00625$).

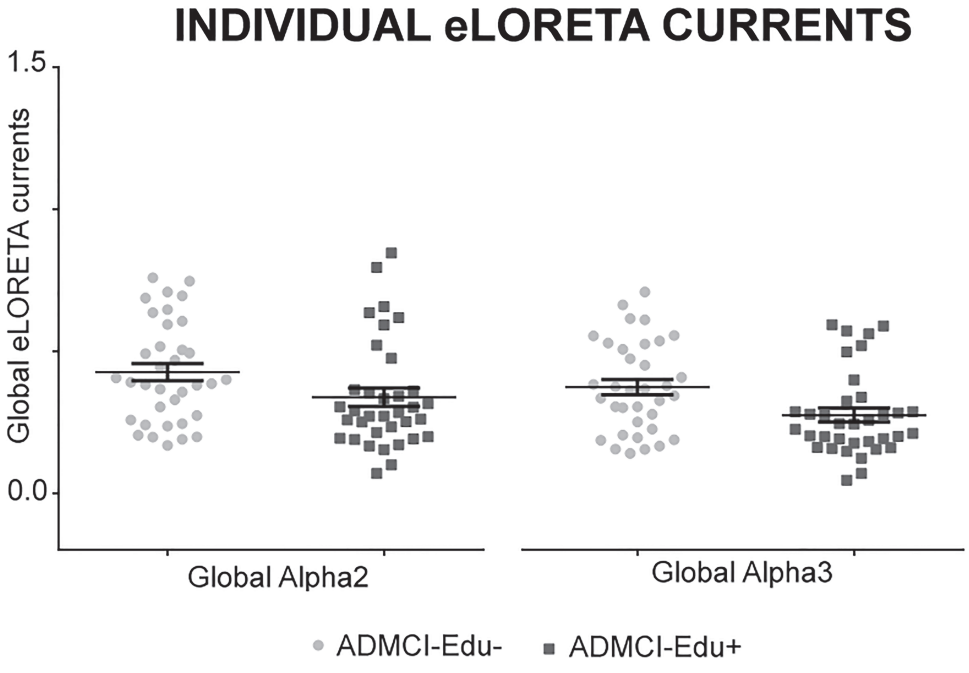

Figure 6. Individual values (log-10 transformed) of the global alpha 2 and alpha 3 normalized eLORETA solutions showing statistically significant ($P < 0.00625$ to have a $P < 0.05$ corrected for multiple post-hoc comparisons) difference between ADMCI-Edu– ($N = 20$) and ADMCI-Edu+ ($N = 20$) subgroups. Noteworthy, the Grubbs' test showed no outliers from those individual values of the eLORETA solutions (arbitrary threshold of $P < 0.001$).

seniors had more ample alpha rhythms in posterior areas as compared to the SMC-Edu– seniors (Babiloni, Lopez, et al. 2020a).

Taken together, the above previous evidence and the present findings suggest that in cognitively unimpaired seniors, a high CR may be associated to a significant synchronization in the activity of diffuse cortical neural populations generating the dominant rsEEG alpha rhythms. This may represent a neuroprotective neurophysiological mechanism. Indeed, several pathological brain processes including AD neuropathology and neurodegeneration are typically related to an opposite feature of rsEEG alpha rhythms, namely an amplitude reduction in those alpha rhythms prominent in posterior areas (Babiloni, Binetti et al. 2006; Babiloni et al. 2013, 2015, 2018a, 2018b; Galluzzi et al. 2016; Jovicich et al. 2019; Marizzoni et al. 2019).

Table 8 Mean values (± SE) of the MRI markers (i.e., volumes of the total gray matter, total white matter, caudate, putamen, pallidum, accumbens, hippocampus, amygdale, and lateral ventricle; cortical thicknesses of the total cortex and entorhinal cortex; white matter hypointensity and lesions) as well as the results of their statistical comparisons (*T*-test on log-10 transformed data; $P < 0.05$ corrected) in the subgroups of ADMCI-Edu– ($N = 35$) and ADMCI-Edu+ ($N = 35$) patients. The volumes were normalized with reference to the total intracranial volume

MRI markers in ADMCI-Edu– and ADMCI-Edu+			
	ADMCI-Edu–	ADMCI-Edu+	*T* test
Global markers			
Normalized WM volume	0.29 ± 0.01	0.30 ± 0.01	$P = 0.3$
Normalized GM volume	0.39 ± 0.01	0.38 ± 0.01	$P = 0.4$
Cortical thickness	4.7 ± 0.1	4.7 ± 0.1	$P = 0.3$
Basal ganglia markers			
Normalized caudate volume	0.0044 ± 0.0001	0.0046 ± 0.0001	$P = 0.3$
Normalized putamen volume	0.0057 ± 0.0001	0.0058 ± 0.0001	$P = 0.5$
Normalized pallidum volume	0.0025 ± 0.0001	0.0026 ± 0.0001	$P = 0.3$
Normalized accumbens volume	0.00056 ± 0.00002	0.00056 ± 0.00002	$P = 0.9$
Mesial temporal markers			
Normalized hippocampus volume	0.0049 ± 0.0001	0.0047 ± 0.0002	$P = 0.2$
Normalized amygdale volume	0.0019 ± 0.0001	0.0019 ± 0.0001	$P = 0.3$
Entorhinal cortical thickness	6.6 ± 0.1	6.4 ± 0.1	$P = 0.2$
Ventricular markers			
Normalized lateral ventricle volume	0.020 ± 0.001	0.022 ± 0.001	$P = 0.3$
Hypointensity/lesion WM markers			
WM hypointensity	2898 ± 365	2461 ± 275	$P = 0.6$
WM lesions	2739 ± 616	2435 ± 538	$P = 0.4$

Notes: ADMCI-Edu– = patients with MCI due to AD and low educational level; ADMCI-Edu+ = patients with MCI due to AD and high educational level. Noteworthy, no significant difference was observed between the 2 ADMCI groups even when a marginal threshold of $P < 0.05$ uncorrected was used.

When considering the above tentative explanation, one should take into account that the hypothesized neurophysiological neuroprotective mechanism may be just one of the neural correlates underpinning the CR. For example, previous structural MRI evidence showed that in relation to SMC seniors with a low CR, those with a high CR were characterized by a larger cortical thickness (Vaqué-Alcázar et al. 2017), which may mitigate brain white matter abnormalities and delay the onset of cognitive deficits along the aging (Mortamais et al. 2014).

Cognitive Reserve and rsEEG Alpha Rhythms in the ADMCI Patients

As a main result of the present study, the ADMCI-Edu+ subgroup (higher education attainment) showed lower alpha source activations topographically widespread as compared to the ADMCI-Edu– subgroup (lower education attainment). In contrast, the other rsEEG frequency bands including delta and theta exhibited no significant effects in relation to the CR. Furthermore, these 2 ADMCI subgroups had matched (1) cerebrospinal AD diagnostic biomarkers, (2) structural MRI measures of brain gray and white matter lesions, and (3) clinical (abilities of daily living, psychiatric symptoms, etc.) and neuropsychological scores. Therefore, we think that the CR effect in maintaining similar clinical manifestations between 2 ADMCI subgroups may be essentially functional. These findings and considerations extend to the prodromal AD stage conclusions based on previous rsEEG evidence observed in SMC seniors at the preclinical AD stage (Babiloni, Lopez, et al. 2020a). Specifically, we previously reported that the SMC seniors with high CR (education attainment) and positivity to the Alzheimer's amyloid-β biomarkers were characterized by less ample rsEEG alpha rhythms in posterior areas as compared to the SMC seniors negative with those biomarkers (Babiloni, Lopez, et al. 2020a).

On the whole, those previous and the present findings suggest that in the ADMCI patients with prodromal AD, a high CR may subtend undefined neurobiological processes able to compensate for a significant disease-related derangement in the synchronization of cortical neural populations generating the rsEEG alpha rhythms. Indeed, thanks to that compensatory mechanism, such a derangement would not proportionally affect patients' clinical status. Indeed, the 2 subgroups of ADMCI patients with lower and higher education attainment did show similar clinical and neuropsychological scores despite the sensitive differences in the rsEEG alpha rhythms.

The present findings complement with previous neuroimaging evidence in AD patients at all stages of the disease.

In structural MRI studies carried out in ADMCI patients, a high CR (i.e., education attainment, reading, and vocabulary measures, etc.) was associated with the following relevant findings: (1) reduced cortical thickness values but paradoxical later clinical progression to dementia (Querbes et al. 2009; Pettigrew et al. 2017); (2) decreased left hippocampus volume and cortical thickness in the right supramarginal gyrus (Arenaza-Urquijo et al. 2013); and (3) decreased volume in the medial prefrontal, anterior cingulate, and orbitofrontal areas (Bartrés-Faz et al. 2019).

In structural MRI studies carried out in ADD patients, a high CR (education attainment) was related to a smaller regional cortical thickness in frontal, temporal, and parietal association areas (Seo et al. 2011) and greater atrophy in temporal gyrus, inferior and superior parietal gyri, and lateral occipital cortex (Liu et al. 2012).

In the same line, previous resting state FDG-PET brain mappings unveiled that a high CR (education attainment) was related to hypometabolism in (1) temporo-parietal and ventral prefrontal areas in Nold seniors with a preclinical AD neuropathology (Ewers et al. 2013). Furthermore,

the hypometabolism was also observed in the precuneus (Franzmeier, Göttler, et al. 2017a; Franzmeier, Duering, et al. 2017b) and a set of regions including posterior parietal and posterior cingulate (Bauckneht et al. 2018) in ADMCI patients.

Furthermore, results of the Alzheimer's disease neuroimaging initiative (ADNI) showed that the CR (education attainment) was not able to predict the cerebral amyloid-β deposition and the metabolic rate in ADMCI patients (Wada et al. 2018).

The results of the present study unveiled that the ADMCI-Edu+ (higher education attainment) and ADMCI-Edu– (lower education attainment) subgroups were characterized by a difference in rsEEG source markers. Namely, the ADMCI-Edu+ subgroup showed lower alpha source activations as compared to the ADMCI-Edu– subgroup. In contrast, the ADMCI-Edu+ and ADMCI-Edu– subgroups exhibited no differences in the following structural MRI markers: (1) the total GM and WM volumes; (2) the total cortical thickness; (3) the volumes of caudate, putamen, pallidum, accumbens, hippocampus, amygdale, and lateral ventricle; (4) the cortical thicknesses of the entorhinal cortex; and (5) the WM hypointensity and hyperintensity as measures of cerebrovascular lesions.

The present results are in line with previous evidence showing that in SMC seniors positive to the diagnostic amyPET markers of AD, those with high CR (education attainment) were characterized by lower rsEEG alpha rhythms but similar structural MRI markers as compared to those with low CR (Babiloni, Lopez, et al. 2020a). The present results are also in line with previous evidence indicating that as compared to the ADMCI patients with low CR, those with similar cognitive deficits and high CR showed a greater resting state FDG-PET hypometabolism in the precuneus (Franzmeier, Göttler, et al. 2017a; Franzmeier, Duering, et al. 2017b; Garibotto et al. 2008) and temporo-parietal associative cortical areas (Garibotto et al. 2008). These CR effects were stronger in ADMCI patients who converted to ADD than the stable ones (Morbelli et al. 2013).

In the present results, the negligible effects of the CR on structural MRI markers might be due to the limited brain atrophy observed in the ADMCI subgroups. Indeed, the CR effects on the brain atrophy were previously reported mainly in ADD patients (Querbes et al. 2009; Sole-Padulles et al. 2009; Teipel et al. 2009; Liu et al. 2012; van Loenhoud et al. 2017). However, the present lack of effects does not mean that MRI markers are irrelevant. Indeed, a previous longitudinal MRI study reported that in high CR patients, the risk for conversion from ADMCI to dementia was predicted by WM lesions (Serra et al. 2015).

Why might EEG markers be more sensitive than MRI markers to the effects of the CR in ADMCI patients? The EEG markers may reflect neural ionic current flows and related voltages at different spatial scales in the brain at an insuperable time resolution (i.e., $<$1 ms). Specifically, they may reflect the synchronization of activity and generation of postsynaptic potentials in several squared centimeters of cortical pyramidal neurons regulating vigilance (resting state), motivation, and cognitive processes (Nunez 2000; Babiloni, Blinowska, et al. 2020b). This synchronization may be induced by several interdependent neural circuits including (1) ascending activating fibers from brainstem and basal forebrain; (2) thalamo-cortical, cortico-thalamic, and cortical local interneurons; and (3) cortico-cortical fibers ensuring longitudinal intrahemispheric and interhemispheric neural transmissions (Nunez 2000; Voytek and Knight 2015; Babiloni, Blinowska, et al. 2020b). In contrast to the EEG markers, structural MRI markers may reflect neuronal apoptosis, tissue damage, synaptic loss, atrophy, neurodegeneration of cortical structures, and cerebrovascular lesions (Frisoni et al. 2010, 2017; Fayed et al. 2012; Filippi et al. 2012). Keeping in mind the above data and considerations, we speculate that in the AD progression, functional compensatory mechanisms underlying the CR might affect earlier neurophysiological oscillatory mechanisms generating the present EEG markers and later the brain neurodegeneration and cerebrovascular lesions detected by MRI markers. Future longitudinal studies will have to test this intriguing speculation.

Cognitive Reserve Mechanism Possibly Affecting rsEEG Alpha Rhythms

At the present early stage of the research, we do not know which CR neurobiological mechanisms may be able to (1) compensate the reduced rsEEG alpha source activations in the ADMCI-Edu+ patients and (2) mitigate the impact of that reduction on individuals' clinical status. Indeed, the CR neurobiological mechanisms are related to both constitutional and environmental factors and operate at various spatial scales in the brain (Arenaza-Urquijo and Vemuri 2020).

Among them, the most probable CR-related mechanisms affecting rsEEG alpha source activations may be those operating at a large spatial macroscale. In this line, it may be speculated that those mechanisms may include the increase in the cortical functional connectivity reported in recent resting state functional MRI studies performed in groups of Nold (Franzmeier, Hartmann, et al. 2018a), ADMCI (Franzmeier, Göttler, et al. 2017a), and ADD (Franzmeier, Düzel, et al. 2018b) individuals. In those studies, as compared to the participants with a low CR (educational attainment), those with a high CR was associated with an increase in the functional connectivity between an anterior circuit spanning prefrontal and premotor areas and other cortical loops involved in general cognition and episodic memory such as default mode and dorsal frontoparietal attention networks (Franzmeier, Göttler, et al. 2017a; Franzmeier, Hartmann, et al. 2018a; Franzmeier, Düzel, et al. 2018b).

Future studies combining rsEEG and resting state functional MRI in ADMCI patients may test whether the high CR (education attainment) may predict the reduction in rsEEG source activations in relation to changes in resting state functional MRI markers of cortical functional connectivity.

Methodological Remarks

The clinical 10–20 electrode montage (i.e., 19 scalp electrodes) adopted for the present rsEEG recordings is generally considered as too low for accurate rsEEG source estimations (Liu et al. 2002; Marino et al. 2016). In that line of reasoning, an optimal spatial sampling would require $>$64 scalp electrodes (Liu et al. 2002; Marino et al. 2016). However, the present findings may be acceptable for the following 2 reasons.

Firstly, rsEEG rhythms show largely dominant low spatial frequency components allowing a valid antialiasing spatial sampling of instantaneous voltage distributions by the mentioned 10–20 electrode montage. This topographically widespread distribution of rsEEG rhythms was unveiled by classical investigations of brain "microstates," defined as quasi-stable topographical patterns of rsEEG voltage maps lasting few seconds each (Lehmann et al. 1987). These patterns typically show 2 very large bipolar voltage centroids of about 10 cm each over the scalp (Khanna et al. 2015; Michel and Koenig 2018). Those large positive and negative voltage centroids may originate in

distributed cortical neural networks revealed by resting state functional MRI (Khanna et al. 2015; Michel and Koenig 2018).

Secondly, the present findings showed that a high CR was related to changes in rsEEG source activations topographically widespread in both Nold and ADMCI subgroups, so possibly overcoming the issue of the spatial resolution.

Another significant methodological limitation is the availability of the rsEEG recordings only at a single data acquisition session, thus preventing the evaluation of the relationship between the CR and rsEEG alpha source activations during the AD progression.

The above methodological limitations motivate resource investments to develop future prospective, longitudinal, and multicenter studies using (1) harmonized EEG hardware systems and clinical protocols; (2) a higher number of exploring scalp electrodes for spatially enhanced rsEEG source estimates; and (3) at least 2 follow-ups capturing the transition to the dementia stage.

Conclusion

It is well-known that Nold and AD seniors with high CR are clinically resistant and resilient to brain neuropathology and neurodegeneration. Here, we tested whether this effect in Nold and ADMCI persons may be associated with changes in the neurophysiological oscillatory mechanisms generating dominant rsEEG alpha rhythms.

As compared to the Nold subgroup with the low CR (education attainment), the Nold subgroup with the high CR showed greater alpha source activations topographically widespread. On the contrary, in relation to the ADMCI subgroup with the low CR, the ADMCI subgroup with the high CR displayed lower alpha source activations topographically widespread. Noteworthy, the other rsEEG bands showed no effect related to the CR. Furthermore, the 2 ADMCI subgroups pointed to similar cerebrospinal AD diagnostic biomarkers, gray and white matter brain lesions, and clinical and neuropsychological scores.

The present findings suggest that the CR, as measured by the education attainment, was related to different changes in dominant rsEEG alpha rhythms in Nold and ADMCI persons. On one hand, the results in the Nold seniors unveiled that the high CR may have a neuroprotective impact by an enhancement in the rsEEG alpha source activations. On the other hand, the results in the ADMCI patients disclosed that the high CR may mitigate the consequences of that reduction on patients' clinical status in a way unrelated to structural brain changes.

The above findings motivate further research to understand the neurobiological and physiological mechanisms underlying the present effects of the CR on rsEEG alpha source activations in Nold and ADMCI persons.

Notes

The present study was developed based on the data of an Italian–Turkish Consortium with some datasets of the FP7-IMI "PharmaCog" (www.pharmacog.org) project. The members and institutional affiliations of the Clinical Units are reported in the cover page of this manuscript. *Conflict of Interest:* None declared.

Funding

In this study, the electroencephalographic data analysis was partially supported by the funds of "Ricerca Corrente" attributed by Italian Ministry of Health to the IRCCS SDN of Naples, IRCCS OASI Maria SS of Troina, and IRCCS San Raffaele Pisana of Rome.

References

Albert MS, DeKosky ST, Dickson D, Dubois B, Feldman HH, Fox NC, Gamst A, Holtzman DM, Jagust WJ, Petersen RC et al. 2011. The diagnosis of mild cognitive impairment due to Alzheimer's disease: recommendations from the National Institute on Aging-Alzheimer's Association workgroups on diagnostic guidelines for Alzheimer's disease. *Alzheimers Dement*. 7:270–279.

Arenaza-Urquijo EM, Molinuevo JL, Sala-Llonch R, Solé-Padullés C, Balasa M, Bosch B, Olives J, Antonell A, Lladó A, Sánchez-Valle R et al. 2013. Cognitive reserve proxies relate to gray matter loss in cognitively healthy elderly with abnormal cerebrospinal fluid amyloid-β levels. *J Alzheimers Dis*. 35: 715–726.

Arenaza-Urquijo EM, Vemuri P. 2018. Resistance vs. resilience to Alzheimer disease: clarifying terminology for preclinical studies. *Neurology*. 90:695–703.

Arenaza-Urquijo EM, Vemuri P. 2020. Improving the resistance and resilience framework for aging and dementia studies. *Alzheimers Res Ther*. 14(12):41.

Arenaza-Urquijo EM, Wirth M, Chételat G. 2015. Cognitive reserve and lifestyle: moving towards preclinical Alzheimer's disease. *Front Aging Neurosci*. 10(7):134.

Babiloni C, Binetti G, Cassetta E, Dal Forno G, Del Percio C, Ferreri F, Ferri R, Frisoni G, Hirata K, Lanuzza B et al. 2006. Sources of cortical rhythms change as a function of cognitive impairment in pathological aging: a multi-centric study. *Clin Neurophysiol*. 117:252–268.

Babiloni C, Carducci F, Lizio R, Vecchio F, Baglieri A, Bernardini S, Cavedo E, Bozzao A, Buttinelli C, Esposito F et al. 2013. Resting state cortical electroencephalographic rhythms are related to gray matter volume in subjects with mild cognitive impairment and Alzheimer's disease. *Hum Brain Mapp*. 34:1427–1446.

Babiloni C, Del Percio C, Boccardi M, Lizio R, Lopez S, Carducci F, Marzano N, Soricelli A, Ferri R, Triggiani AI et al. 2015. Occipital sources of resting-state alpha rhythms are related to local gray matter density in subjects with amnesic mild cognitive impairment and Alzheimer's disease. *Neurobiol Aging*. 36:556–570.

Babiloni C, Del Percio C, Lizio R, Noce G, Lopez S, Soricelli A, Ferri R, Pascarelli MT, Catania V, Nobili F et al. 2017a. Abnormalities of cortical neural synchronization mechanisms in subjects with mild cognitive impairment due to Alzheimer's and Parkinson's diseases: an EEG study. *J Alzheimers Dis*. 59:339–358.

Babiloni C, Del Percio C, Lizio R, Noce G, Cordone S, Lopez S, Soricelli A, Ferri R, Pascarelli MT, Nobili F et al. 2017b. Abnormalities of cortical neural synchronization mechanisms in patients with dementia due to Alzheimer's and Lewy body diseases: an EEG study. *Neurobiol Aging*. 55:143–158.

Babiloni C, Del Percio C, Lizio R, Noce G, Lopez S, Soricelli A, Ferri R, Pascarelli MT, Catania V, Nobili F et al. 2018a. Abnormalities of resting state cortical EEG rhythms in subjects with mild cognitive impairment due to Alzheimer's and Lewy body diseases. *J Alzheimers Dis*. 62:247–268.

Babiloni C, Del Percio C, Lizio R, Noce G, Lopez S, Soricelli A, Ferri R, Pascarelli MT, Catania V, Nobili F et al. 2018b. Functional cortical source connectivity of resting

state electroencephalographic alpha rhythms shows similar abnormalities in patients with mild cognitive impairment due to Alzheimer's and Parkinson's diseases. *Clin Neurophysiol*. 129:766–782.

Babiloni C, Lopez S, Del Percio C, Noce G, Pascarelli MT, Lizio R, Teipel SJ, González-Escamilla G, Bakardjian H, George N et al. 2020a. Resting-state posterior alpha rhythms are abnormal in subjective memory complaint seniors with preclinical Alzheimer's neuropathology and high education level: the INSIGHT-preAD study. *Neurobiol Aging*. 90:43–59.

Babiloni C, Blinowska K, Bonanni L, Cichocki A, De Haan W, Del Percio C, Dubois B, Escudero J, Fernández A, Frisoni G et al. 2020b. What electrophysiology tells us about Alzheimer's disease: a window into the synchronization and connectivity of brain neurons. *Neurobiol Aging*. 85:58–73.

Bartrés-Faz D, González-Escamilla G, Vaqué-Alcázar L, Abellaneda-Pérez K, Valls-Pedret C, Ros E, Grothe MJ. 2019. Characterizing the molecular architecture of cortical regions associated with high educational attainment in older individuals. *J Neurosci*. 39:4566–4575.

Bennett DA, Arnold SE, Valenzuela MJ, Brayne C, Schneider JA. 2014. Cognitive and social lifestyle: links with neuropathology and cognition in late life. *Acta Neuropathol*. 127:137–150.

Brown LM, Schinka JA. 2005. Develpment and initial validation of a 15-item informant version of the geriatric depression scale. *Int J Getriatr Psychiatry*. 20:911–918.

Buchman AS, Bennett DA. 2012. Amyloid pathology in persons with "normal" cognition. *Neurology*. 78:228–229.

Bauckneht M, Chincarini A, Piva R, Arnaldi D, Girtler N, Massa F, Pardini M, Grazzini M, Efeturk H, Pagani M et al. 2018. Metabolic correlates of reserve and resilience in MCI due to Alzheimer's disease (AD). *Alzheimers Res Ther*. 3(10):35.

Caltagirone C, Gainotti G, Carlesimo GA, Parnetti L, eil gruppo per la standardizzazione della batteria per il deterioramento mentale. 1995. Batteria per la valutazione del deterioramento mentale (parte I): descrizione di uno strumento di diagnosi neuropsicologica. *Arch Psicol Neurol Psichiatr*. 56:461–470.

Ewers M, Insel PS, Stern Y, Weiner MW, Alzheimer's Disease Neuroimaging Initiative (ADNI). 2013. Cognitive reserve associated with FDG-PET in preclinical Alzheimer disease. *Neurology*. 80:1194–1201.

Fayed N, Modrego PJ, Salinas GR, Gazulla J. 2012. Magnetic resonance imaging based clinical research in Alzheimer's disease. *J Alzheimers Dis*. 31(Suppl 3):5–18.

Filippi M, Agosta F, Frisoni GB, De Stefano N, Bizzi A, Bozzali M, Falini A, Rocca MA, Sorbi S, Caltagirone C et al. 2012. Magnetic resonance imaging in Alzheimer's disease: from diagnosis to monitoring treatment effect. *Curr Alzheimer Res*. 9:1198–1209.

Fleck JI, Arnold M, Dykstra B, Casario K, Douglas E, Morris O. 2019. Distinct functional connectivity patterns are associated with social and cognitive lifestyle factors: pathways to cognitive reserve. *Front Aging Neurosci*. 11:310.

Fleck JI, Kuti J, Mercurio J, Mullen S, Austin K, Pereira O. 2017. The impact of age and cognitive reserve on resting-state brain connectivity. *Front Aging Neurosci*. 9:392.

Folstein MF, Folstein SE, McHugh PR. 1975. Mini-mental state. A practical method for grading the cognitive state of patients for the clinician. *J Psychiatr Res*. 12:189–198.

Franzmeier N, Göttler J, Grimmer T, Drzezga A, Áraque-Caballero MA, Simon-Vermot L, Taylor ANW, Bürger K, Catak C, Janowitz D et al. 2017a. Resting-state connectivity of the left frontal cortex to the default mode and dorsal attention network supports Reserve in Mild Cognitive Impairment. *Front Aging Neurosci*. 9:264.

Franzmeier N, Duering M, Weiner M, Dichgans M, Ewers M, Alzheimer's Disease Neuroimaging Initiative (ADNI). 2017b. Left frontal cortex connectivity underlies cognitive reserve in prodromal Alzheimer disease. *Neurology*. 88:1054–1061.

Franzmeier N, Hartmann J, Taylor ANW, Araque-Caballero MÁ, Simon-Vermot L, Kambeitz-Ilankovic L, Bürger K, Catak C, Janowitz D, Müller C et al. 2018a. The left frontal cortex supports reserve in aging by enhancing functional network efficiency. *Alzheimers Res Ther*. 10:28.

Franzmeier N, Düzel E, Jessen F, Buerger K, Levin J, Duering M, Dichgans M, Haass C, Suárez-Calvet M, Fagan AM et al. 2018b. Left frontal hub connectivity delays cognitive impairment in autosomal-dominant and sporadic Alzheimer's disease. *Brain*. 141:1186–1200.

Freedman M, Leach L, Kaplan E, Winoucur G, Shulman KJ, Delis DC. 1994. *Clock drawing. A neuropsichological analysis*. New York: Oxford University Press.

Frisoni GB, Fox NC, Jack CR Jr, Scheltens P, Thompson PM. 2010. The clinical use of structural MRI in Alzheimer disease. *Nat Rev Neurol Feb*. 6:67–77.

Frisoni GB, Boccardi M, Barkhof F, Blennow K, Cappa S, Chiotis K, Démonet JF, Garibotto V, Giannakopoulos P, Gietl A et al. 2017. Strategic roadmap for an early diagnosis of Alzheimer's disease based on biomarkers. *Lancet Neurol*. 16:661–676.

Galluzzi S, Marizzoni M, Babiloni C, Albani D, Antelmi L, Bagnoli C, Bartres-Faz D, Cordone S, Didic M, Farotti L et al. 2016. Clinical and biomarker profiling of prodromal Alzheimer's disease in workpackage 5 of the innovative medicines initiative Pharma cog project: a 'European ADNI study. *J Intern Med*. 279:576–591.

Garibotto V, Borroni B, Kalbe E, Herholz K, Salmon E, Holtoff V, Sorbi S, Cappa SF, Padovani A, Fazio F et al. 2008. Education and occupation as proxies for reserve in aMCI converters and AD: FDG-PET evidence. *Neurology*. 71:1342–1349.

Giovagnoli A, Del Pesce M, Mascheroni S, Simoncelli M, Laiacona M, Capitani E. 1996. Trail making test: normative values from 287 normal adult controls. *Ital J Neurol Sci*. 17:305–309.

Hampel H, Mesulam MM, Cuello AC, Khachaturian AS, Vergallo A, Farlow MR, Snyder PJ, Giacobini E, Khachaturian ZS. 2019. Revisiting the cholinergic hypothesis in Alzheimer's disease: emerging evidence from translational and clinical research. *J Prev Alzheimers Dis*. 6:2–15.

Jovicich J, Babiloni C, Ferrari C, Marizzoni M, Moretti DV, Del Percio C, Lizio R, Lopez S, Galluzzi S, Albani D et al. 2019. Two-year longitudinal monitoring of amnestic mild cognitive impairment patients with prodromal Alzheimer's disease using topographical biomarkers derived from functional magnetic resonance imaging and electroencephalographic activity. *J Alzheimers Dis*. 69:15–35.

Khanna A, Pascual-Leone A, Michel CM, Farzan F. 2015. Microstates in resting-state EEG: current status and future directions. *Neurosci Biobehav Rev*. 49:105–113.

Klimesch W, Doppelmayr M, Russegger H, Pachinger T, Schwaiger J. 1998. Induced alpha band power changes in the human EEG and attention. *Neurosci Lett*. 244:73–76.

Klimesch W, Doppelmayr M, Russegger H, Pachinger T. 1996. Theta band power in the human scalp EEG and the encoding of new information. *Neuroreport*. 7:1235–1240.

Klimesch W. 1999. EEG alpha and theta oscillations reflect cognitive and memory performance: a review and analysis. *Brain Res Rev*. 29:169–195.

Lehmann D, Ozaki H, Pal I. 1987. EEG alpha map series: brain micro-states by space-oriented adaptive segmentation. *Electroencephalogr Clin Neurophysiol*. 67:271–288.

Liu AK, Dale AM, Belliveau JW. 2002. Monte Carlo simulation studies of EEG and MEG localization accuracy. *Hum Brain Mapp*. 16:47–62.

Liu Y, Julkunen V, Paajanen T, Westman E, Wahlund LO, Aitken A, Sobow T, Mecocci P, Tsolaki M, Vellas B et al. 2012. Education increases reserve against Alzheimer's disease—evidence from structural MRI analysis. *Neuroradiology*. 54:929–938.

Marino M, Liu Q, Brem S, Wenderoth N, Mantini D. 2016. Automated detection and labeling of high-density EEG electrodes from structural MR images. *J Neural Eng*. 13:056003.

Marizzoni M, Ferrari C, Macis A, Jovicich J, Albani D, Babiloni C, Cavaliere L, Didic M, Forloni G, Galluzzi S et al. 2019. Biomarker matrix to track short term disease progression in amnestic mild cognitive impairment patients with prodromal Alzheimer's disease. *J Alzheimers Dis*. 69:49–58.

Mattsson N. 2011. CSF biomarkers in neurodegenerative diseases. *Clin Chem Lab Med*. 49:345–352.

Michel CM, Koenig T. 2018. EEG microstates as a tool for studying the temporal dynamics of whole-brain neuronal networks: a review. *NeuroImage*. 180:577–593.

Monllau A, Pena-Casanova J, Blesa R, Aguilar M, Bohm P, Sol JM, Hernandez G. 2007. Diagnostic value and functional correlations of the ADAS-cog scale in Alzheimer's disease: data on NORMACODEM project. *Neurologia*. 22:493–501.

Morbelli S, Nobili F. 2014. Cognitive reserve and clinical expression of Alzheimer's disease: evidence and implications for brain PET imaging. *Am J Nucl Med Mol Imaging*. 4:239–247.

Morbelli S, Perneczky R, Drzezga A, Frisoni GB, Caroli A, Berckel BN van, Ossenkoppele R, Guedj E, Didic M, Brugnolo A et al. 2013. Metabolic networks underlying cognitive reserve in prodromal Alzheimer disease: a European Alzheimer disease consortium project. *J Nucl Med*. 54:894–902.

Morris JC. 1993. The clinical dementia rating (CDR): current version and scoring rules. *Neurology*. 43:2412–2414.

Mortamais M, Portet F, Brickman AM, Provenzano FA, Muraskin J, Akbaraly TN, Berr C, Touchon J, Bonafé A, le Bars E et al. 2014. Education modulates the impact of white matter lesions on the risk of mild cognitive impairment and dementia. *Am J Geriatr Psychiatry*. 22:1336–1345.

Novelli G, Papagno C, Capitani E, Laiacona M, Vallar G, Cappa SF. 1986. Tre test clinici di ricerca e produzione lessicale. Taratura su soggetti normali. *Arch Psicol Neurol Psichiatr*. 47: 477–506.

Nunez PL. 2000. Toward a quantitative description of large-scale neocortical dynamic function and EEG. *Behav Brain Sci*. 23:371–98; discussion 399–437.

Pascual-Marqui RD. 2007. Discrete, 3D distributed, linear imaging methods of electric neuronal activity. Part 1: exact, zero error localization. *Math Phys*. 1–16. http://arxiv.org/pdf/0710.3341.

Perneczky R, Drzezga A, Diehl-Schmid J, Schmid G, Wohlschläger A, Kars S, Grimmer T, Wagenpfeil S, Monsch A, Kurz A. 2006. Schooling mediates brain reserve in Alzheimer's disease: findings of fluoro-deoxy-glucose-positron emission tomography. *J Neurol Neurosurg Psychiatry*. 77:1060–1063.

Pettigrew C, Soldan A, Zhu Y, Wang MC, Brown T, Miller M, Albert M, BIOCARD Research Team. 2017. Cognitive reserve and cortical thickness in preclinical Alzheimer's disease. *Brain Imaging Behav*. 11:357–367.

Pfurtscheller G, Lopes da Silva FH. 1999. Event-related EEG/MEG synchronization and desynchronization: basic principles. *Clin Clin Neurophysiol*. 110:1842–1857.

Pietrini P, Furey ML, Alexander GE, Mentis MJ, Dani A, Guazzelli M, Rapoport SI, Schapiro MB. 1999. Association between brain functional failure and dementia severity in Alzheimer's disease: resting versus stimulation PET study. *Am J Psychiatry*. 156:470–473.

Querbes O, Aubry F, Pariente J, Lotterie JA, Démonet JF, Duret V, Puel M, Berry I, Fort JC, Celsis P. 2009. Alzheimer's disease neuroimaging initiative. Early diagnosis of Alzheimer's disease using cortical thickness: impact of cognitive reserve. *Brain*. 132:2036–2047.

Reed BR, Mungas D, Farias ST, Harvey D, Beckett L, Widaman K, Hinton L, DeCarli C. 2010. Measuring cognitive reserve based on the decomposition of episodic memory variance. *Brain*. 133:2196–2209.

Reitan RM. 1958. Validity of the trail making test as an indicator of organic brain damage. *Percept Mot Skills*. 8:271–276.

Rentz DM, Mormino EC, Papp KV, Betensky RA, Sperling RA, Johnson KA. 2017. Cognitive resilience in clinical and preclinical Alzheimer's disease: the Association of Amyloid and tau burden on cognitive performance. *Brain Imaging Behav*. 11:383–390.

Rey A. 1968. *Reattivo della figura complessa*. Firenze: Organizzazioni Speciali.

Roe CM, Xiong C, Miller JP, Morris JC. 2007. Education and Alzheimer disease without dementia: support for the cognitive reserve hypothesis. *Neurology*. 68:223–228.

Rosen WG, Mohs RC, Davis KL. 1984. A new rating scale for Alzheimer's disease. *Am J Psychiatry*. 141:1356–1364.

Rosen WG, Terry RD, Fuld PA, Katzman R, Peck A. 1980. Pathological verification of ischemic score in differentiation of dementias. *Ann Neurol*. 7:486–488.

Seo SW, Im K, Lee J-M, Kim ST, Ahn HJ, Go SM, Kim S-H, Na DL. 2011. Effects of demographic factors on cortical thickness in Alzheimer's disease. *Neurobiol Aging*. 32:200–209.

Serra L, Musicco M, Cercignani M, Torso M, Spanò B, Mastropasqua C, Giulietti G, Marra C, Bruno G, Koch G et al. 2015. Cognitive reserve and the risk for Alzheimer's disease: a longitudinal study. *Neurobiol Aging*. 36:592–600.

Solé-Padullés C, Bartrés-Faz D, Junqué C, Vendrell P, Rami L, Clemente IC, Bosch B, Villar A, Bargalló N, Jurado MA et al. 2009. Brain structure and function related to cognitive reserve variables in normal aging, mild cognitive impairment and Alzheimer's disease. *Neurobiol Aging*. 30:1114–1124.

Stern Y, Alexander GE, Prohovnik I, Stricks L, Link B, Lennon MC, Mayeux R. 1995. Relationship between lifetime occupation and parietal flow: implications for a reserve against Alzheimer's disease pathology. *Neurology*. 45:55–60.

Stern Y, Arenaza-Urquijo EM, Bartrés-Faz D, Belleville S, Cantilon M, Chetelat G, Ewers M, Franzmeier N, Kempermann G, Kremen WS et al. 2018. Reserve, resilience and protective factors PIA empirical definitions and conceptual frameworks workgroup. Whitepaper: defining and investigating cognitive reserve, brain reserve, and brain maintenance. *Alzheimers Dement*. S1552-5260:33491–33495.

Stern Y. 2012. Cognitive reserve in ageing and Alzheimer's disease. *Lancet Neurol*. 11:1006–1012.

Teipel SJ, Meindl T, Wagner M, Kohl T, Bürger K, Reiser MF, Herpertz S, Möller HJ, Hampel H. 2009. White matter microstructure in relation to education in aging and Alzheimer's disease. *J Alzheimers Dis*. 17:571–583.

Valenzuela MJ, Sachdev P. 2006. Brain reserve and cognitive decline: a non-parametric systematic review. *Psychol Med*. 36:1065–1073.

van Loenhoud AC, Wink AM, Groot C, Verfaillie SCJ, Twisk J, Barkhof F, van Berckel B, Scheltens P, van der Flier WM,

Ossenkoppele R. 2017. A neuroimaging approach to capture cognitive reserve: application to Alzheimer's disease. *Hum Brain Mapp*. 38:4703–4715.

Vaqué-Alcázar L, Sala-Llonch R, Valls-Pedret C, Vidal-Piñeiro D, Fernández-Cabello S, Bargalló N, Ros E, Bartrés-Faz D. 2017. Differential age-related gray and white matter impact mediates educational influence on elders' cognition. *Brain Imaging Behav*. 11:318–332.

Voytek B, Knight RT. 2015. Dynamic network communication as a unifying neural basis for cognition, development, aging, and disease. *Biol Psychiatry*. 77:1089–1097.

Wada M, Noda Y, Shinagawa S, Chung JK, Sawada K, Ogyu K, Tarumi R, Tsugawa S, Miyazaki T, Yamagata B, et al. 2018. Alzheimer's Disease Neuroimaging Initiative. Effect of education on Alzheimer's disease-related neuroimaging biomarkers in healthy controls, and participants with mild cognitive impairment and Alzheimer's disease: a cross-sectional study. *J Alzheimers Dis* 63:861–869.

Wan L, Huang H, Schwab N, Tanner J, Rajan A, Lam NB, Zaborszky L, Li CR, Price CC, Ding M. 2019. From eyes-closed to eyes-open: role of cholinergic projections in EC-to-EO alpha reactivity revealed by combining EEG and MRI. *Hum Brain Mapp*. 40:566–577.

Watson YI, Arfken CL, Birge SJ. 1993. Clock completion: an objective screening test for dementia. *J Am Geriatr Soc*. 41:1235–1240.

Wechsler D. 1987. *Manual for the Wechsler memory scale-revised*. San Antonio (TX): The Psychological Corporation.

Zahodne LB, Manly JJ, Brickman AM, Siedlecki KL, Decarli C, Stern Y. 2013. Quantifying cognitive reserve in older adults by decomposing episodic memory variance: replication and extension. *J Int Neuropsychol Soc*. 19:854–862.

Zahodne LB, Manly JJ, Brickman AM, Narkhede A, Griffith EY, Guzman VA, Schupf N, Stern Y. 2015. Is residual memory variance a valid method for quantifying cognitive reserve? A longitudinal application. *Neuropsychologia*. 77:260–266.